Degradation mechanisms in organic photovoltaic devices

Grossiord, Nadia; Kroon, Jan M.; Andriessen, Ronn; Blom, Paul W. M.

Published in:
Organic Electronics

DOI:
10.1016/j.orgel.2011.11.027

Organic Electronics 13 (2012) 432–456

Contents lists available at SciVerse ScienceDirect

Organic Electronics

journal homepage: www.elsevier.com/locate/orgel

Review

Degradation mechanisms in organic photovoltaic devices

Nadia Grossiord [a,*], Jan M. Kroon [b], Ronn Andriessen [a], Paul W.M. Blom [a,c]

[a] Holst Centre/TNO, High Tech Campus 31, 5656 AE Eindhoven, The Netherlands
[b] Energy Research Centre of The Netherlands (ECN), P.O. Box 1, 1755 ZG Petten, The Netherlands
[c] Zernike Institute for Advanced Materials, University of Groningen, Nijenborgh 4, 9747 AG Groningen, The Netherlands

ARTICLE INFO

Article history:
Received 30 September 2011
Received in revised form 24 November 2011
Accepted 27 November 2011
Available online 14 December 2011

Keywords:
Organic photovoltaics
Degradation mechanisms
Stability
Lifetime

ABSTRACT

In the present review, the main degradation mechanisms occurring in the different layer stacking (i.e. photoactive layer, electrode, encapsulation film, interconnection) of polymeric organic solar cells and modules are discussed. Bulk and interfacial, as well as chemical and physical degradation mechanisms are reviewed, as well as their implications and external or internal triggers. Decay in *I–V* curves in function of time is usually due to the combined action of sequential and interrelated mechanisms taking place at different locations of the device, at specific kinetics. This often makes the identification of specific root causes of degradation challenging in non-model systems. Additionally, constant development and refinement in terms of type and combination of materials and processes render the ranking of degradation mechanisms as a function of their probability of occurrence and their detection challenging.

However, it clearly appears that for the overall stability of organic photovoltaic devices, the actual photoactive layer, as well as the properties of the barrier and substrate (e.g. cut of moisture and oxygen ingress, mechanical integrity), remain critical. Interfacial stability is also crucial, as a modest degradation at the level of an interface can quickly and significantly influence the overall device properties.

1. Introduction

Presently, about 65–70% of electricity consumed in the world is derived from the combustion of fossil fuels, such as oil, coal and natural gas [1]. Over the past decade, the field of renewable energy production experienced a rapid growth as a result of the increased awareness regarding the limited availability of fossil fuels [2], the negative impact on the environment induced by their use [3], as well as the high price volatility of oil.

In the field of alternative energy production, photovoltaics (PVs) have a significant potential as it is the only portable, readily available and renewable source of electricity. Some numbers to give an idea of this potential: the total annual solar energy striking the surface of the Earth is estimated to be 63×10^{15} W [4], which is a thousand times higher than the total energy requirement of the earth population (i.e. about 15×10^{12} W in 2009). This requirement is expected to considerably increase within the coming 40 years due to the overall growth of the population, as well as to an increase of the quality of life and of the access to consumption for an expanding part of the world population [5].

Producing electricity from renewable resources, such as (sun) light, is essentially cost driven. The major PV technology commercially available nowadays is crystalline silicon (c-Si). It accounted for about 90% of the whole PV market share in 2008, and is mainly based on costly batch-to-batch semi-conductor processing production techniques. The average annual growth of c-Si PV production capacity was 30–50% over the last 10 years [6]. Although these numbers seem large, the global share of PV technology in electricity generation is still marginal. The main reason remains the high overall cost of electricity

* Corresponding author. Tel.: +31 (0)40 40 20 454; fax: +31 (0)40 40 20 699.
E-mail address: nadia.grossiord@tno.nl (N. Grossiord).

1566-1199/$ - see front matter © 2011 Elsevier B.V. All rights reserved.
doi:10.1016/j.orgel.2011.11.027

production. Depending on the local market landscape and geographical factors, electricity produced using PV installations is still a factor two to four more expensive compared to electricity produced by traditional electricity plants like coal and gas centrals, as well as hydroelectric and nuclear power plants [7,8].

In order to circumvent this issue, efforts have been devoted to the development of alternative low-cost thin film PV manufacturing technologies [9–11]. In particular, an interesting new generation of PV cells, the so-called Organic PhotoVoltaic (OPV) devices involve the use of semi-conductive polymers. These materials are very promising as their properties can be easily tailored. Additionally, they are soluble in many organic solvents, allowing deposition by large scale solution based printing or coating processes. This should bring the cost of (O)PV devices manufacturing economically competitive. Additionally, light, flexible and (semi-) transparent OPV cells and modules offer the prospect to be produced with a large freedom of design, opening ways to new applications such as portable charging of small devices which could, for example, be integrated in clothing and bags. Other possible applications include the integration of OPV products to retractable shades, tents, carport covers, windows, etc. [12].

However, there are still some improvements to be achieved in order to fulfil all requirements in terms of three key parameters, namely efficiency, lifetime and cost for future commercialization [12–14]. It is agreed that, as long as a product falls short to address at least one of these key parameters, it remains confined to niche markets.

Although the OPV market is still in its infancy, production, integration, and installation costs of this type of products are expected to remain very low compared to existing technologies [10]. However, efficiency and lifetime are still substantially lower than the ones of inorganic cells [15]. Regarding this first point, constant developments in the fields of materials, device design, as well as in cell and module configuration, make expectations to succeed in manufacturing commercial products with power conversion efficiencies as high as at least 10% (value corresponding to theoretical and experimental predictions [16,17]) reasonable. Even if this value remains lower than the 25–30% efficiency levels exhibited by inorganic solar cells, 8–10% efficiency would be acceptable for a viable commercial product if this value is compensated by significantly lower manufacturing costs. The second point, life expectancy, which indirectly determines the cost of the energy provided by the technology, is still poor compared to inorganic silicon-based solar cells which can last 25 years. Consequently, it appears that significant improvements have to be made in terms of lifetime to make OPV technologically attractive for e.g. mass production and commercialization. To do so, knowledge of types and degradation mechanisms that can occur is a prerequisite.

The present review is aimed at providing an overview of the different degradation mechanisms occurring in (flexible) OPV cells and modules based on *polymer:fullerene* active materials. First, the basic design of OPV cells will be presented and examples given of the type of materials required to prepare the currently "standard" layouts which are mostly described and studied in literature. Subsequently, potential degradation mechanisms will be listed. Main triggers and consequences of these degradation mechanisms will be included in this description, as well as a list of characterization methods used to detect, localize and study them. Although part of the literature mentioned gives the detail of the degradation of benchmark materials used in the current "standard" OPV device layout, the concepts treated can easily be extended to a much broader range of materials. Finally, results of representative stability tests published in literature or presented at conferences, as well as initiatives aiming at standardizing this type of tests, will be discussed.

1.1. Introduction to organic (polymer) photovoltaics and working principle

The term "photovoltaic" has been coined from the Greek 'photo' which means light and voltaic meaning electric from the name of the Italian Volta (who gave his name to the electro-motive unit Volt).

The photovoltaic effect was first recognized in 1834 by the French physicist Antoine-Henri Becquerel, who later conjointly won the Nobel Prize of Physics with Pierre and Marie Curie for their discovery of radioactivity. Becquerel reported for the first time that exposure to electro-magnetic radiation of certain materials, namely platinum electrodes covered with silver chloride or silver bromide in water, could lead to the production of a small electric current (photochemical effect) [18,19]. Only 50 years later, the first reports on photoconductivity of a solid-state system, selenium, were made [20,21]. The beginning of the 20th century saw the dawn of the research in photoconductivity on organic compounds, with the study of anthracene [22,23].

Since the first production of synthetic polymers, e.g. bakelite [24] and synthetic rubber by emulsion polymerization, in the first half of the 20th century [25], polymeric materials (i.e. large molecules, each of which includes a large number of repeating structural units) have taken an increasing importance at all levels at all stages of our life, mainly because of their superior materials properties, versatility, low density and easy processing. Conduction along polymer backbones was reported as early as the 60s [26–29]. In 1977, A.J. Heeger, A.G. MacDiarmid and H. Shirakawa, who shared the Nobel Prize in Chemistry in 2000, greatly popularized this subject by reporting a significant conductivity increase by oxidative doping of polyacetylene [30,31]. It is generally agreed that the mechanism of conductivity in conjugated polymers is based on the motion through hopping of charged carriers between conjugated fragments of the polymer framework. These charges can be positive (holes) or negative (electrons) and are the results of oxidation and reduction of the polymer, respectively [32,33].

For inorganic semiconductors, the exciton binding energy is small in comparison to the thermal energy (kT, for which k is the Boltzmann constant and T the temperature) at room temperature. As a result, free charges are easily created at room temperature while the material is excited [34]. On the contrary, for an organic semiconductor, a bound electron–hole pair, a so-called exciton, of which

the binding energy is about one order of magnitude higher than kT (of the order of 0.5–2 eV [35–38]), is created upon light absorption [39–41]. As a result, charge separation with creation of free charge carriers is unlikely at room temperature and recombination occurs [42]. That is why the first OPV devices based on a single layer of an organic *p*-conductor (so-called Schottky diodes) exhibited very poor performances [43,44]. Consequently, a donor–acceptor interface between materials with different electron affinities and ionization potentials is required in order to trigger exciton dissociation. When an exciton is formed at the electron acceptor (A)- electron donor (D) interface, the material with lower ionization potential accepts the hole (electron donor), whereas the 2nd material with the larger electron affinity accepts the negative charge carrier (electron acceptor) [45]. In the case of for example a polymer D and fullerene based A, the charge transfer is highly efficient and stable as it occurs much faster than the competing recombination processes [45–47]. This concept of heterojunction PV [48] opened new ways to prepare OPV based on polymer-fullerene, [47] polymer–polymer [49,50] and polymer-nanoparticle [51] heterojunctions, with increased performances. Since then, the efforts devoted towards the use of conductive polymers for this specific application have never faded [52].

The general operation principle of an OPV cell can be summarized as follow:

- At first, photons of (sun) light meet the first interface of the device and must go through several (transparent) layers in order to reach the photoactive layer (PAL). A fraction of these photons are absorbed by the electron donor D, which induces electron excitation from its Highest Occupied Molecular Orbital (HOMO) to its Lowest Unoccupied Molecular Orbital (LUMO). The fraction of photons absorbed depends on the thickness of the PAL (the thicker the layer is, the more photons are collected – for a majority of conjugated polymers, most photons are absorbed within the first 100–500 nm of the PAL depending of its light penetration profile [33]), the optical properties (e.g. transparency) of the layers covering this photoactive layer (PAL) and on the energy range of photons which can be absorbed by D. Typical strategies to broaden the energy range of absorbed photons involves tuning the band gap of the electron donor/photon absorber, e.g. by reducing its band gap value and its HOMO level values, both aiming at increasing the absorption of red photons present in a significant fraction of energy of the solar spectrum [16]. Furthermore, the absorption by the active layer can be improved by using acceptors as 6,6-phenyl-C_{71}-butyric acid methyl ester ([70] PCBM) that can also absorb a significant part of the (visible) solar spectrum, preferentially a part that is complementary to the absorption of the donor [53]. An other option is to construct tandem or double junction cells. The latter are typically made of two electron donor materials with non-overlapping absorption spectra stacked or mixed in double junction cells [54,55].
- Upon the absorption of a photon an exciton is formed. In order to guarantee an efficient process, the exciton needs to be dissociated before it decays. As explained above this dissociation takes place at the interface of the donor/acceptor blend. Since the diffusion length of an exciton in a A/D bi-layer system is very small (in the order of 5–10 nm [56,57]), the external quantum efficiency (η_{EQE}), defined as the number of electrons produced by a PV cells for each photon absorbed, is therefore ultimately limited by the number of photons that can be absorbed within an exciton diffusion length from the A/D interface. That is why the PAL is usually made of an interpenetrating network formed from a phase-segregated mixture of A and D, of which the separated domain size must be in the order of 10 nm to minimize exciton recombination (so-called bulk heterojunction BHJ) [50]. After dissociation of the exciton a hole in the donor phase is formed together with an electron in the acceptor phase. When the distance between the electron and the hole is typically 1 nm, their Coulomb binding energy is still in the order of ~0.5 eV. As a result after dissociation of the exciton the formed electron–hole pair is still bound and needs to be dissociated into free charge carriers. The dissociation process of the bound e–h pair is electric field and temperature dependent, and also depends on the local morphology [58].
- Finally the positive and the negative charge carriers must move towards the opposite electrodes via bicontinuous interpenetrating networks. To do so, the electrons and the holes must "travel" throughout the bulk of the PAL via percolating paths of the A and D materials, respectively [59,60]. The charge carrier mobility and resulting speed is strongly influenced by the properties of the A and D phases, notably by the amount of defects and impurities, organization/crystallinity, etc. [61].
- Once they have reached the electrodes, the free charges are collected and passed into the outer circuit to generate the device photocurrent. The charge collection efficiency mainly depends on the energy level matching at the metal/polymer interface and on interfacial defects [58,62].

2. State of the art – OPV cells and modules

Since OPV technology is still in its early development stages, precisely defining a "typical" OPV cell layout is not yet possible. For the same reason, the materials selection for the different electro-active layers is still unsettled.

Basically, the photoactive layer, where the conversion from light to electricity takes place, is sandwiched in between a pair of contacts or electrodes, at least one of which being transparent, see Fig. 1. The term electrode refers to a layer that provides a medium for delivering photogenerated power to an external circuit or for providing a bias voltage to the device. Electrodes can be made of a single material or of a combination of several compounds (e.g. either a mono- or multilayer system or a composite material). These three main layers constitute the cell itself.

Nowadays, the work horse device design for bulk heterojunction cells is based on a glass substrate on top of which Indium Tin Oxide (ITO) has been sputtered. The whole is then covered by a film made of a polymer mixture of a

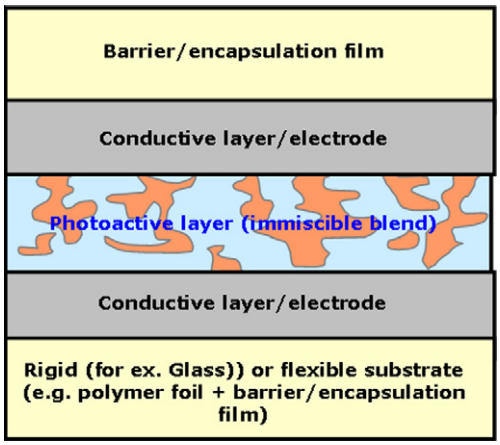

Fig. 1. Schematic representation of an OPV bulk-heterojunction cell structure.

conductive poly(3,4-ethylenedioxythiophene) polymer doped with poly(styrenesulfonate) (PEDOT:PSS), being the hole-collecting electrode (characterized by a high work function value). The PEDOT:PSS hole collecting layer or anode is subsequently coated with the PAL. Currently, the most widely used photo-active blend based on an interpenetrating electron D/A immiscible blend is 6,6-phenyl-C_{61}-butyric acid methyl ester ([60] PCBM) or 6,6-phenyl-C_{71}-butyric acid methyl ester ([70] PCBM) as electron acceptor [53,63] and poly(3-hexylthiophene) (P3HT) as electron donor [64–68]. Initially, poly(2-methoxy-5-(3′,7′-dimethyloctyloxy-1,4-phenylenevinylene)) (MDMO-PPV) and other PPV derivatives were used due to their large availability. Since 2003–2004, P3HT is preferred due to its higher hole mobility (greatly due to its polymeric chain packing ability), alkyl side groups that favor solubilization in most common solvents, good polymer-PCBM co-solubility, as well as larger overlap between its absorption spectrum and the solar emission spectrum. [33,69–72] In laboratory devices, PEDOT:PSS and PAL deposition is almost always achieved by spin coating.

A low work function metal cathode (LiF/Al, Ca/Al, Ba/Al or Al – electron collection) is evaporated on top of the PAL blend to finalize the solar cell. In the majority of the cases, OPV cells are prepared and characterized in a glove box (inert, moisture- and oxygen-free atmosphere).

Next to this "conventional" regular device architecture, so-called inverted bulk-heterojunction solar cells are also widely studied. As its name indicates, the layer sequence of the latter is inverted, i.e. the cathode is the electrode in contact with the substrate and the anode is located on top of the device. The most widely studied stack is similar to the one of the corresponding conventional cell. The cathode is often made of an ITO layer sputtered on a glass substrate, on top of which an electron transport layer made of *n*-type metal oxides (such as ZnO or TiO_x) is deposited. Afterwards the PAL, most often made of P3HT and PCBM blend, is spin coated. Finally, the whole is covered by a top anode made of a metal possessing a high work function such as Ag, usually deposited by thermal evaporation.

Tandem or multi-junction cells, in which several single-junction cells, usually with non-overlapping absorption spectra, are stacked over each other in order to broaden the absorption band of the cell, are also gaining more and more attention [54].

As already previously mentioned, the PAL of a bulk-heterojunction cell can be made of different types of materials, namely polymer/polymer, polymer/fullerene derivatives or polymer/nanoparticles (such as carbon nanotubes, quantum dots, ZnO, etc.) blends as well as a blend of small molecules. In the framework of this paper, we will mainly focus on the systems in which the photoactive layer consists of polymers used as D and/or A, and fullerene derivatives used as A.

Since solar cells are used in ambient atmosphere, they generally need to be protected on both sides by an extra layer that prevents or, more exactly, considerably slows down oxygen and moisture diffusion into the OPV device. It has indeed been shown that electrodes placed on both sides of the cell are gas and moisture permeable [73] and thus do not hinder OPV cell degradation. The environmental sensitivity of OPV dictates the need of barrier layers with (very) low moisture and oxygen permeation. The exact value of the gas transmission rates required in order to guarantee a minimum lifetime for commercial applications is not precisely known since the latter is function of the specific end application of the product [12]. Current oxygen and moisture barriers are typically multilayered structures alternating thick organic and thin non-organic (typically oxide or nitride) layers used to encapsulate OLEDs. Their water and oxygen transmission rates are of the order of 10^{-6}–10^{-4} g m^{-2} day^{-1} and 10^{-3} cm^3 m^{-2} day^{-1} atm^{-1}, respectively [74]. The exact requirements to be specifically fulfilled for OPV are not very well defined yet. As a result, most information dealing with this part of the OPV stack was collected in literature dealing with substrates and barrier films designed for flexible electronic devices such as light-emitting diodes and flexible displays.

In order to lower the production costs of OPV cells roll-to-roll fabrication is an attractive technology. However, this requires the substrates to be flexible, meaning that glass for the time being cannot be used as substrate. In view of the recent developments in the field of roll-able and flexible glass, this might change in the future [75]. But so far, this technology is not sufficiently developed.

As for the interconnections required by the module manufacturing, only a few companies, institutes or universities effectively study or publish about OPV modules. As a result, most information used for this part comes from silicon-based PV technologies. Nevertheless, considering the similarity of design between flexible (amorphous) Si thin film PV and flexible OPV, it is very likely that the latter will benefit from the development in the field of module making of this more mature technology.

3. Overview degradation mechanisms in OPV cells

In the first part of this Section 1, a number of possible degradation mechanisms, and how these can affect the OPV properties and performance, are discussed. Subsequently, an overview of characterization techniques to study these degradation mechanisms will be given. In the

second part, degradations occurring at various parts of the OPV device will be reviewed: each layer will be considered individually and finally the interface between two layers, either at the edge (sealant) or at the interconnections (e.g. between cells and/or the module and the "outside world"), will be discussed.

3.1. Introduction

Measuring the current–voltage characteristics of a cell or module enables the evaluation of most of its photovoltaic performance as well as its electric behavior. Fig. 2 displays the typical current–voltage (I–V) characteristics of an illuminated solar cell, which is usually operated between open circuit and short circuit conditions. This type of curve is obtained by applying a range of voltages across the cell under illumination, and measuring the corresponding photocurrent.

Charge collection is driven by the built-in electric field in the device. The overall efficiency of a solar cell, which is defined as the maximum power produced by the photovoltaic device divided by the incident light power, can be expressed as follows:

$$\eta = \frac{V_{oc} J_{sc} FF}{P_{in}} \quad (1)$$

where V_{oc} is the open circuit voltage (i.e. the voltage V when $I = 0$), J_{sc} the short circuit current (i.e. the photogenerated current collected at the electrodes when $V = 0$ (in A/m^2, often expressed in mA/cm^2)), FF the fill factor (blue square in Fig. 2). P_{in} refers to the incident light power, which is equal to the irradiance (in W/m^2) multiplied by the area of the solar cell (in m^2) and which is usually standardized.

In the most general definition of the word, degradation refers to the process of impairing certain properties of a given material. In the particular case of OPV cells, degradation ultimately leads to a decrease/loss in performance. Consequently, measuring the changes in J_{sc}, V_{oc} or FF values as a function of time can give some hints regarding the type of degradation taking place.

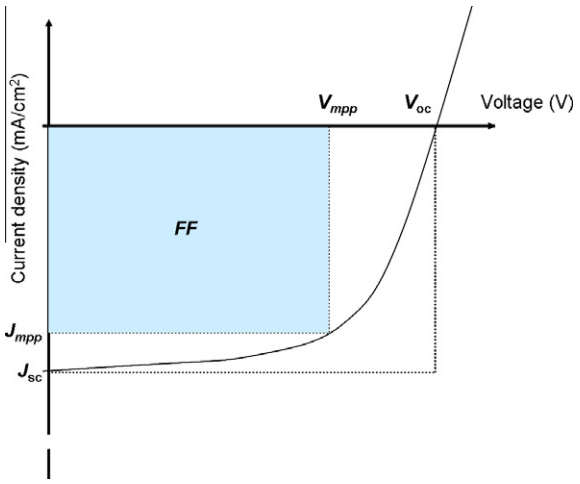

Fig. 2. Typical current–voltage curve of an (O)PV cell. The short circuit current (J_{sc}), the open circuit voltage (V_{oc}), the fill factor (FF), the voltage (V_{mpp}), and the current (J_{mpp}) at maximum power point are shown.

J_{sc} is determined by the external quantum efficiency, η_{EQE}, which "summarizes" the efficiency of all basic processes of an OPV cell, namely light absorption, exciton dissociation at the A/D interface, and free charge transfer and collection to the electrodes. η_{EQE} is defined as the fraction of incident photons which are effectively converted into electrical current and can be calculated by using the following equation:

$$\eta_{EQE} = \eta_A \, \eta_{ED} \, \eta_{CC} \quad (2)$$

where η_A is the light absorption efficiency, i.e. the probability of photon absorption, η_{ED} the exciton diffusion efficiency, i.e. the fraction of photogenerated excitons which reaches the A–D interface (the dissociation efficiency of the bound electron–hole pair is function of the PAL nature and composition [76,77]), and, η_{CC} the carrier collection efficiency, i.e. the probability that a free charge carrier reaches an electrode.

An J_{sc} decrease during the cell operation corresponds to a decrease of the number of charges collected at the electrodes, which may be caused by various degradations impacting photon absorption, charge dissociation, transport to the electrodes as well as PAL/electrode transfer (see Table 1).

V_{oc} is mainly determined by the energy difference between the HOMO of the electron donor and the LUMO of the electron acceptor (E_{gap}). It is also a function of other parameters, such as the temperature, as can be seen in the following equation:

$$V_{oc} = \frac{E_{gap}}{q} - \frac{kT}{q}\left(\frac{(1-P)\gamma N_c^2}{PG}\right) \quad (3)$$

where q is the elementary charge, k the Boltzmann's constant, T the temperature, G the generation rate of bound electron–hole pairs, P the dissociation probability of a bound electron–hole pair into free charges, γ the Langevin recombination constant, and N_c the effective density of states. The reader can refer to Ref. [78] for more detailed information.

As can be seen from Eq. (3), modification (degradations a.o.) of PAL components and/or electrodes leading to a change of the values of the HOMO of the electron donor and/or LUMO of the electron acceptor can significantly affect the value of V_{oc}.

The fill factor FF is the ratio of the maximum extractable power to the maximum theoretical power output:

$$FF = \frac{V_{mpp} \, J_{mpp}}{V_{oc} \, J_{sc}} \quad (4)$$

V_{mpp} (resp. J_{mpp}) represents the voltage (resp. current) at the maximum power point. Following the evolution over time of FF provides information about the quality of charge extraction in the device, the evolution of the interfaces between the different layers of the stacking, and the charge transport through each layer. In other words, FF represents the overall quality of the diode as a device and is determined by intrinsic processes as the recombination losses, the formation of space-charges due to unbalanced

Table 1
Correspondence between the main OPV degradation pathways and their impact on the main characteristics of OPV cells. This list is based on results reported in references cited afterwards in the present article.

Parameter affected (generally reduced) and key factors determining it	Possible causes
FF	Reduced interfacial charge transfer efficiency between the different layers (e.g. degradation of the quality of the PAL/electrode interface)
Serial resistance (R_s)	Deterioration of charge transport in the layers (e.g. bulk material degradation)
Shunt resistance (R_{sh})	Presence of shunts and shorts
V_{oc}	Reduction of the PAL: electrode interface
	Lowering of the "effective" band gap of the PAL blend materials
Energy difference between the HOMO of the electron donor and the LUMO of the electron acceptor	Electrode W_f change
	Presence of shorts
J_{sc} – Light absorption efficiency η_A	Chemical degradation of the electron donor (e.g. loss of polymer conjugation) of the PAL
Molecular architecture of the polymer (=band gap)	Loss of transparency of the stack through which the photon must travel to reach the PAL
Thickness of the photoactive layer (PAL)	
J_{sc} – Exciton dissociation efficiency η_{ED}	Decrease of the D/A interface area/ increase of the blend domains (above the diffusion length of the exciton)
Match of band gap (HOMO (electron acceptor A)/LUMO (electron donor D) levels)	
D/A blend morphology	
J_{sc} – Carrier (transport and) collection efficiency η_{CC}	Loss of percolating paths due to blend reorganization
	Degradation of the electrode/PAL interface due to for instance electrode degradation
	Change in energy levels of the cell components
Percolation pathway to electrodes (D to hole collecting electrode and A to electron collecting electrode)	Cracks
Organization of transportation pathways of the A and of the D materials (e.g. crystallinity)	Layer delamination
Device architecture (e.g. electrode-PAL A/D blend interface area)	Degradation of material leading to decrease of charge carrier mobilities/formation of traps

transport. Additionally, it is largely influenced by two extrinsic factors, namely (see Scheme 1 which shows the equivalent circuit of a non-ideal PV cell under illumination):

- the shunt resistance, R_{sh}, which generally reflects the degree of leakage current through the whole device, and which is often linked to imperfections during the production process,

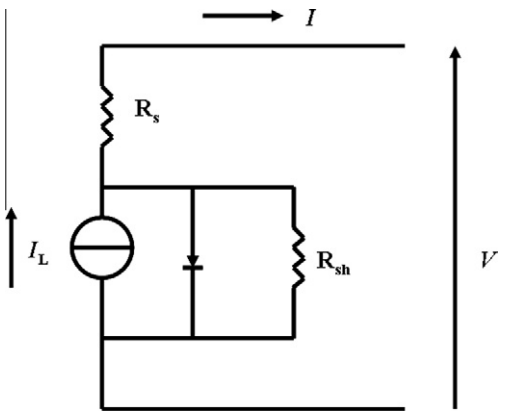

Scheme 1. Equivalent circuit of a real PV cell (one-diode model). This circuit corresponds to an imperfect current generator, with shunt (R_{sh}) and series resistance (R_s). I_L represents an ideal cell, i.e. a current source of which the intensity depends on the illumination. (scheme adapted from Ref. [42]).

- the serial resistance, R_s, which is notably due to the resistivity of all materials of the OPV stack, the resistivity of the metallization (such as the busbars), as well as by the contact resistance between the various materials (especially at the PAL/electrode interface).

Generally, large serial resistances, due to e.g. degradation of the bulk of a material or of the quality of the electrode/PAL interface, as well as too small parallel resistance (due to shunts) tend to reduce the *FF* value.Table 1 gives a (non-exhaustive) list of the main degradation mechanisms affecting the *I–V* device characteristics.

However, as shown in Table 1, since several causes can lead to the same trend, it is generally arduous to specifically pinpoint the exact cause of degradation by only studying the *I–V* characteristics as a function of time of OPV devices. That is why cause diagnostic is often facilitated by studying model systems of incomplete cells (e.g. study of one layer or of the degradation of compounds taken individually) and/or by using other characterization techniques on complete devices in addition to *I–V* measurements.

The main techniques used and described in literature are mentioned in Table 2, as well as the suitable type of samples, on which they can be used, i.e. on complete or non-complete devices.

Physical and/or chemical degradation modes of (flexible) OPV devices can be divided in two main categories:

- intrinsic degradation due to changes in the characteristics of the interface between layers of the stacking owing to internal modification of the materials used,

Table 2
List of characterization techniques used to study OPV degradation. For each technique, it is specified whether the technique can be directly used on the cell seen as a whole (highlighted in bold) or whether it is restricted to the study of samples made of an individual layer(s) of an incomplete cell. The references provided are those of published works (cited in other parts in this article) which utilize the characterization techniques mentioned to study (degradation of) OPV cells and/or modules. This list of publication does not have the presumption to be exhaustive, but rather to give relevant examples of the use of the mentioned techniques to study OPV device degradation.

Test/characterization technique	Sample used	Remarks
Spectral response and *I–V* measurements	Whole cell/module	Integral measurement – no extraction of precise information regarding the exact location and nature of the degradation
Scanning microscope for semi-conductor characterization (SMSC) [169]	Whole cell	Local information and measurement of J_{sc} current density enabled -2D mapping possible
Infrared imaging- lock-in thermography [249,250,260,261]	Whole cell/module	
Optical microscopy [234,247]	Layer/whole cell	
Confocal (fluorescent) microscopy [115,234]	Layer	Possibility to obtain 3D structures of the samples – used to study OLED degradation in the references mentioned
Scanning near field optical microscopy [133]	Layer	
Atomic Force Microscopy (AFM) [115,234]	Layer or top layer of a complete cell	Mostly used to characterize individual layer surfaces. Can be used on an OPV cell when top electrode studied
Scanning Electron Microscopy [115,234,247]	Layer, top or cross section of a complete cell/module	Mostly used to characterize individual layer surfaces. Can be utilized to image the cross section or the top of a complete OPV cell – used to study OLED degradation in the articles mentioned
Transmission Electron Microscopy (TEM)	Layer [146]	
	TEM tomography [262] – layer	3D imaging of the PAL layer reported (when sufficient contrast)
	Whole cell [263]	Focused Ion Beam technique used to prepare cross-sectional samples
UV–Vis spectroscopy [85–87,143,235,238]	Layer	
Infrared (IR) spectroscopy [86,87,90]	Layer	
Electrochemical Impedance spectroscopy [264]	Layer	
Fluorescence spectroscopy [86,115]	Layer/ sample can be a whole cell	
Auger electron spectroscopy [160]	Layer	
Electron Energy Loss Spectroscopy (EELS) [160]	Layer	
Core-level photoabsorption spectroscopy [265]	Layer	
X-ray Diffraction (XRD) [143]	Layer	
X-ray Photoelectron Spectrometry [227]	Layers and whole cells	Used in combination with TOF-SIMS to get quantitative data
Rutherford backscattering spectrometry [193]	Layer	Used to study OLED degradation in the articles mentioned
X-ray reflectometry [162,163]	Whole cell – study of the interface between layers	
Photo-luminescence [143]	Layer	
TOF-SIMS [115,166,227]	Layer/ whole cell	
Differential Scanning Calorimetry (DSC) [238]	Layer	Analytical technique to study polymer phase transitions
Size Exclusion Chromatography (SEC) [81]	Layer	Used more specifically to detect and characterize polymer chain scission
Electron microprobe [247]	Layer	
Kelvin probe [160]	Layer	Electrode work function measurement

- extrinsic degradation caused by changes in the cell behavior induced by external triggers, such as water, oxygen, electromagnetic radiations (UV, visible light, IR, ...), etc. The latter is strongly linked to the quality and stability in properties of the encapsulation system, namely the barrier, the substrate and the type of edge sealing used.

In the following section, possible OPV degradation mechanisms will be listed, layer by layer, starting with the PAL, continuing with the electrodes and the barrier/encapsulation systems, ending with the degradations more specific to cells connected together in modules (interconnections and hot spots).

3.2. Degradations taking place in the PAL

3.2.1. Chemical degradation of PAL compounds

3.2.1.1. Polymeric compounds (electron donor and acceptor). Conjugated conducting polymers typically exhibit an alternating single-double bond structure, which is responsible for the formation of a highly delocalized π-electron system with large electronic polarizability. As a result, absorption of photons within the visible light region

and electrical charge transport are enabled. Charge transport occurs along the short, undisrupted fragments of the polymeric chain by thermally-induced hopping. [79,80] Polymer crystallization promotes charge transport since it usually decreases the amount of (energetical) disorder, contributing in this way to the performance improvement of OPV cells [61].

Any chemical reaction affecting the degree of conjugation (disruption of the π conjugation leads to a decrease of the UV–Vis absorbance) and/or ordering of the polymer chains (e.g. due to chain scission) contribute to cell degradation as they affect charge transport. In all the cases, J_{sc} decreases, which induces a drop of the OPV cell efficiency.

Light is one of the main triggers for polymer degradation. Photochemical degradation of the conjugated polymer and its relation to the overall cell performance has received much attention. Among the mechanisms reported are:

- photobleaching of the polymer which results in a disruption of the π-conjugation,
- photooxidation, which can lead to disruption of the π-conjugation and/or chain scission (the latter being due to e.g. ring opening). Furthermore, in many cases carbonyl groups are formed that are very efficient exciton quenchers. Due to this quenching many excitons are lost before they can reach the interface with the acceptor prior to their dissociation,
- photodoping, corresponding to the (reversible) formation of a weakly bound donor–acceptor charge transfer complex D + A = $[D^{\delta+} A^{\delta-}]$. The latter is an efficient excitation quencher,
- free radical attack initiated by photolysis of metallic impurities which is usually followed by chain scission and cross-linking.

3.2.1.2. Photochemical polymer degradation. Similarly to other conjugated molecules, PPV derivatives and poly(3-alkylthiophenes) (P3AT) possess a low photochemical stability, which induces reduced cell operating lifetime. The exact way in which degradation occurs is still under discussion. One of the widely accepted mechanisms of photo-oxidation and thermo-oxidation of P3HT in solution claims that degradation originates from singlet oxygen photosensitisation [81]. Once formed, the singlet oxygen undergoes a Diels–Alder cycloaddition with the thienyl unit of P3HT, ultimately forming an unstable endo-peroxide. The latter subsequently decomposes into sulfine and ketone, among others, which leads to disruption of the π-conjugation. Alternatively, the P3HT side chain can also be oxidized via a free-radical oxidation route, thus forming hydroxyl and carbonyl adducts. This may sometimes lead to cross-linking evidenced e.g. by a loss of solubility in toluene [82]. For the bulk polymer it was clearly demonstrated by Manceau et al. that singlet oxygen is most probably the main intermediate responsible for the degradation [83,84]. Based on the identification of degradation products by IR and UV spectroscopy, i.e. carbonyl- and sulfur moieties which come from the degradation of the side chains (α-carbon atom of the hexyl group of P3HT which is the chemically weakest C–H bond) and of the backbone (S-ring) of the polymer, respectively, Manceau et al. list three types of degradation paths: (i) the H abstraction reaction of alkoxy radicals leading to the formation of an α-unsaturated alcohol (mechanism 1 of scheme 2), (ii) the cage reaction of alkoxy radicals with OH′ leading to the formation of an aromatic ketone (mechanism 2); the latter is unstable when irradiated at wavelengths lower than 400 nm and undergoes a Norrish photolysis, leading to the formation of aromatic carboxylic acid groups and alkyl radicals oxidized into aliphatic acids, and (iii) β-scission leading to the formation of an aromatic aldehyde that rapidly oxidizes into carboxylic acids (mechanism 3). Additionally, the S atoms present in the polymer backbone can first be oxidized into sulfoxides, then to sulfones that decompose into carboxylic acids, see scheme 3. The consequences of all these reactions are conjugation loss and/or chain scissions that lead to UV–Vis absorbance decrease and hole mobility reduction (the latter being notably due to deep-trap formation) [85]. Interestingly, at least in the case of MDMO-PPV, it seems that slower, trap-limited hole transport is to a larger extent responsible for the J_{sc} decrease than photobleaching [85]. All this results in efficiency decrease and reduced device operational lifetime.

Hintz and his coworkers carried out a systematic study of the influence of environmental factors, namely oxygen, light and moisture, on the photodegradation of neat P3HT [86]. They found out that limited, short-term exposure of the polymer to only one of these degradation triggers only causes small irreversible damage. On the contrary, since P3HT UV-triggered degradation is catalyzed by the presence of H_2O and O_2, exposure of P3HT to for example both UV and oxygen was found to lead to severe damage of the polymer structure and hence important deterioration of its properties. Interestingly, Hintz et al. evidenced that the lower the P3HT regioregularity, the faster the degradation.

Manceau and his coworkers recently studied the relationship between structure and stability of a large range of conjugated polymers relevant for OPV. From this systematic study, they could identify which donor and acceptor building blocks of the polymer backbone were the most stable, see Fig. 3. They also found that, regardless of their exact chemical natures, keeping the amount of side groups of the π-conjugated polymer backbone as low as possible was beneficial towards polymer stability [87].

Importantly, it has been shown by several researchers that conjugated polymer photodegradation (of MDMO-PPV, MEH-PPV and P3HT among others), in presence or absence of oxygen, is mitigated and its kinetics seriously reduced up to a few orders of magnitude when the D polymer is mixed with an A fullerene derivative [83,88–92]. This behavior has been explained by both radical scavenging of the fullerene derivative molecule and its ability to quench the P3HT singlet state.

Additionally, V_{oc} decrease (involving overall OPV cell performance decrease) [93–95] may occur upon polymer doping. In the case of *p*-type doping a Schottky diode with the cathode is formed, and the band bending with its corresponding electric field is then limited only to the depletion region of the diode, leading to V_{oc} loss. It has been found that

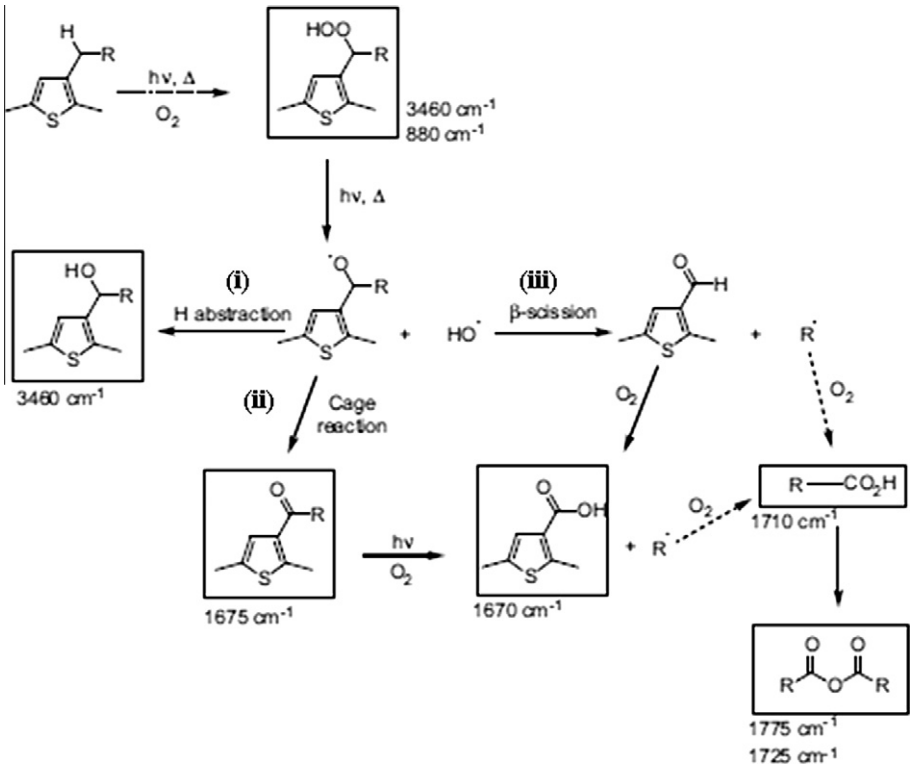

Scheme 2. Oxidation mechanism of the P3HT alkyl side chain (Reproduced with permission of Ref. [83]. Copyright 2009 Elsevier Ltd.).

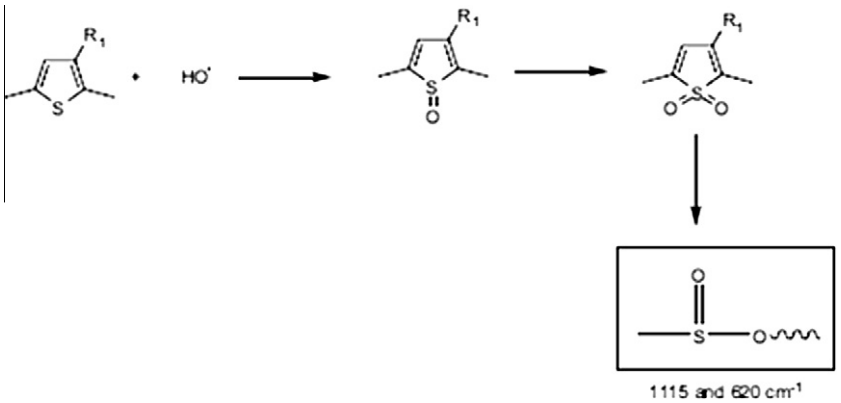

Scheme 3. Oxidation mechanism of the sulfur atom of the thiophene ring (Reproduced with permission of Ref. [83]. Copyright 2009 Elsevier Ltd.).

the *p*-doping of P3HT corresponds to a slow physical adsorption of oxygen molecules on the polymer chain, forming weak contact charge transfer complexes, and is strongly accelerated by light, even at low oxygen pressure [96,97]. In the absence of polymer damage caused e.g. by photooxidation from UV exposure, this oxygen *p*-doping is *fully* reversible upon thermal annealing. Dedoping kinetics are considerably enhanced when the temperature is raised to the polymer glass transition (T_g) which induces polymer chain motions and promotes oxygen release [98].

Usually, even in the absence of oxygen and moisture, (photo)chemical stability of conjugated polymers might be affected by the presence of some types of impurities, i.e. residues of metal catalysts and others reagents, which result from the polymer synthesis and purification and/or doping [72,99,100]. Over the past years, several improvements in polymer or small molecule purification [101,102], as well as in polymer synthesis [103,104], were reported. In the latter case, Gregg and his coworkers demonstrated that the decrease in *p*-type defects induced by treating P3HT with

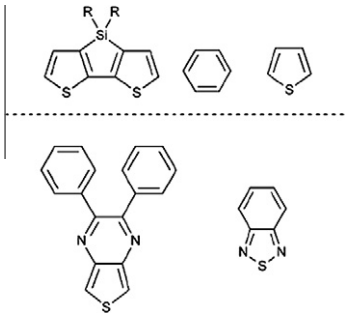

Fig. 3. Most stable donor (top) and acceptor (bottom) units identified in the study of Manceau and his coworkers in Ref. [87], namely (from left to right and from top to bottom): Si-cyclodithiophene, benzene, thiophene, thienopyrazine, and benzothiadiazole (From Ref. [87]. Reprinted with the permission of the Royal Society of Chemistry).

electrophiles or nucleophiles significantly enhanced polymer stability against photodegradation.

3.2.1.3. Non-polymeric compounds (electron donor and acceptor). In inert atmosphere, fullerene and fullerene derivatives are expected to be thermally stable at the operating temperature of the OPV cell, i.e. about 80 °C, according to TGA measurements performed in inert atmosphere and in air [105,106].

Exposure to oxygen lowers the conductivity of fullerene films. Upon oxygen uptake, the electron mobility is reduced by several orders of magnitude because the intercalated oxygen acts as an electron trap [107]. It was reported by Hamed and his coworkers that this effect can be partially reversed by annealing of the C_{60} films in vacuum at 160–180 °C (note that reversibility of the process involves the *absence* of C–O covalent bond formation). However, the degree of "recovery" after annealing of the fullerene films in terms of conductivity and activation energy was smaller when the films had been brought in contact with oxygen under illumination [108]. It has indeed been reported several times that (UV) light enhances oxygen diffusion through the interstitial voids in the fullerene lattice, as well as formation of C–O and/or inter-fullerene C–C bonds [108,109].

Additionally, oxygen uptake favors exciton quenching in the fullerene itself caused by anionic oxygen associated with fullerenes [110].

The main mechanism affecting the fullerene cage properties and integrity is oxidation. Residual oxygen can already be present in the OPV bulk (introduction during device manufacturing and/or contamination from ITO) or reach the inner layers of the OPV device by diffusing from "outside" through the electrodes and encapsulation films. Oxidation itself proceeds via addition of oxygen to the fullerene molecules to form epoxidic species (C_{60} > O, i.e. two different C atoms, each of them linked to one O atom by a single bond) [111] and C_{60}═O (C═O double bond) [112–114]. C–O single bond formation was reported at temperatures in the range of 100 °C, which is higher than the expected device working *T*, but which can possibly be reached during processing. Fullerene cages which are linked with a single bond to atomic oxygen were reported to further decompose and polymerize after 1000 h of heating at 80 °C [113], which may be similar to conditions when using these solar cells in hot climates and can be detrimental to cell performances. On the other hand, the formation of C═O double bonds, leading to cage opening, was observed at *T* in the order of 200–300 °C. However, these *T* are unlikely to be reached during device manufacturing and operational life [114]. Note that fullerene samples, once they have been in contact with oxygen, will oxidatively polymerize upon thermal treatment, even when no additional oxygen is present. This polymerization is much accelerated when it occurs in an oxygen-containing environment [114].

In the particular case of (photo)oxidation of fullerene C_{60} due to the diffusion of oxygen through the pinholes of the cathode, Norrman and co-workers reported that the expansion of C_{60} led to protrusion around the pinholes of the cathode, leading therefore to increased pinhole size coupled with oxygen ingress increase and hence amplification of the effect (resulting in a vicious circle) [115].

According to Könenkamp et al. only 1–10% of the oxygen incorporated in a C_{60} film did effectively induce oxidation reactions [116]. In all the cases, chemical degradation of the A fullerene derivative leads to alteration of its structure, which can then not fulfil its role properly any more, promoting in this way a decrease of the cell efficiency.

An important point to mention is that a significant part of work focussing on the study of PAL component degradation (especially in the case of the study of the polymer degradation) is not carried out on a complete OPV cell, but only on thin layers or on solutions of a given polymer, which is most of the time relevant in order to get fundamental understanding and an accurate picture of the degradation mechanism paths effectively taking place. However, these results may not always give a truthful image of what really takes place in the complete device as other compounds present in the OPV cell layout can strongly influence polymer degradation mechanisms and/or kinetics. As an example, it has been reported several times that mixing conjugated polymers with fullerenes may significantly hinder degradation processes [83,88–91].

3.2.1.4. Prevention of the PAL component chemical degradation. According to results discussed in the previous section, it clearly appears that processing the PAL in an oxygen-poor atmosphere, at relatively low temperature, contributes to the prevention of PAL component degradation. Furthermore, using a suitable encapsulation system in order to hinder oxygen ingress during the operational life of the device can help to significantly increase the lifetime of the device.

In addition, some choices can be made to extent the OPV device lifetime: use of components which are less prone to degradation upon contact with oxygen and moisture (for example, polymers with more stable monomer units, possessing as few as possible side groups), use of "additives" (e.g. PCBM in combination with P3HT), optimization of the polymerization (e.g. tuning of the regioregularity of the synthesized polymer, choice of polymerization routes leading to little residual impurities) and of the possible subsequent purification steps.

3.2.2. Degradation of the D/A morphology of the PAL

3.2.2.1. Description of the degradation of the D/A morphology. In a bulk heterojunction cell, the PAL blend morphology is a key parameter to control the performance of the OPV cells [67]. Photocurrent generation requires uniform A/D blending with domain sizes in the order of about twice the exciton diffusion length, whereas charge transport requires continuous paths from the D/A interface to the electrodes. PAL blend morphology and D/A phase separation occurring during film formation are strongly influenced by the way the PAL has been deposited, e.g. the choice of the solvent system in which both compounds are dissolved, the deposition technique (such as spin coating or ink jet printing), the temperature of the substrate and of the solution during deposition, the drying conditions, the layer thickness, the relative ratio and concentration of the compounds, as well as the molecular weight and regioregularity of the polymer(s) chosen if applicable, a.o. [117–124]. After PAL deposition during OPV cell preparation, the blend morphology may not be optimized yet. That is why an additional thermal annealing step is often applied to the cell after PAL or electrode deposition in order to fine-tune the morphology of the PAL blend in terms of domain size (in the order of 20 nm), donor/acceptor distribution, percolating paths, and, if applicable, (polymer) crystallization that favours transport of photogenerated charges [66,125–127]. This step consists of heating the cell for a fixed time in order to force the PAL blend to phase separate until it reaches an optimum morphology. In all the cases, once the optimum morphology is obtained, it is desirable that the system remains 'frozen' since any further reorganization is very likely to induce worsening of the system efficiency. Spatial reorganization of the polymer blend typically occurs at temperatures higher than the glass transition of the PAL components [128]. However, due to the unavoidable molecular weight distribution of the polymer and/or the possible presence of oligomers resulting from the polymerization, spatial blend reorganisation can be observed at temperatures much lower than the tabulated T_g value. Additionally, diffusion of low molecular weight components, such as the fullerene molecules results in accelerated phase segregation and in the formation of large crystalline aggregates (leading to reduction of D/A interface and possible percolation path disruption) [67,127,129–132]. As an example, PCBM clustering can be observed and monitored upon thermal annealing of MDMO-PPV- and P3HT-based solar cells [132,133]. In the specific case of P3HT/PCBM blends, the morphology of films cast from solvents is the result of a dual crystallization behavior in which the crystal formation is hindered (or controlled) by the second compound, potentially making this blend more thermally stable than amorphous MDMO-PPV/PCBM blends [128]. The thermal annealing step can sometimes be avoided in some cases by using additives (such as polar solvents or small molecules) [134–138] or by drying the PAL under solvent vapor saturated atmosphere (so-called solvent assisted annealing) [134,139].

Considering that the operating temperature of a solar cell placed outside can be as high as 80–95 °C in hot climatic conditions [140–142], it cannot be completely excluded that blend reorganization may in some cases take place during the working life of a cell when the T_g of one of the blend components is lower than the cell highest possible working temperature. Spatial reorganization of the immiscible blend leads to clustering of the two compounds of the blend because of phase separation. As a result, the interfacial area between the two compounds of the blend decreases, which lowers exciton dissociation and charge transport. Moreover, clustering of the two phases leads to a decrease of percolating paths used by the charges to reach the electrode [118,131,143]. Interestingly, Zhao et al. [128] recently reported that P3HT/PCBM blends with a 1:1 weight ratio of each compound (which corresponds to the order of magnitude of ratios known to lead to well-performing cells [118,119,144]) exhibit single T_gs of about 40 °C or less (the P3HT used in the study possessed a relatively low average M_w of 35,000 g mol^{-1}, with a polydispersity of 1.8), therefore making this kind of cells inherently unstable in regular outdoor operating conditions.

Similarly to the studies of chemical degradation of the PAL compounds, most of the works focussing on the study of the PAL blend phase separation are not carried out on a complete OPV cell, but on the PAL considered separately, in particular when characterization techniques such as transmission electron microscopy (TEM) are used [134]. This may sometimes lead to an inaccurate description of the blend morphology of the photoactive layer as the presence of the top or bottom electrode may impact blend movements and surface characteristics, notably roughness [145], or influence morphology evolution due to specific interactions between the electrode and photoactive layers [88].

3.2.2.2. Prevention of the degradation of the D/A morphology. Strategies to increase the long-term thermal stability of the PAL morphology, and thus minimize or suppress further phase separation after processing, consist of using sufficiently high T_g donor/acceptor pairs [143,146,147] and compatibilizers which reduce the interfacial energy between immiscible components of the condensed phase [148]. Cross-linking of the PAL has also proven to be successful. [149–151] Even if it has had limited success until now, mainly due to charge quenching between A and D, another possible route consists of positioning A and D in the same polymer backbone, either by incorporating A moieties in the D polymer backbone (randomly or at the ends of the chain), or by synthesizing block copolymers that can self-assemble into highly stable ordered nanostructures through microphase separation [152,153]. The latter can be either A–D block copolymers or block copolymers of which one block preferably and strongly interacts with A [154]. On the one hand, this strategy may tackle the problem of phase segregation and ensure effective electron transfer under all conditions. On the other hand, it has been suggested that charge extraction becomes more difficult, which may explain why D–A copolymer systems have yet yield efficiencies that compete with those found the discrete D–A material counterpart [155].

3.3. Degradation of the electrodes

Most OPV cells made nowadays possess two types of electrodes: (i) a conducting metal layer (mostly Al, Ag

or Au) as the rear electrode, and (ii) a conductive transparent metal oxide as the front electrode allowing the light to reach the PAL. The conversion efficiency of OPV cells is strongly determined by the performance of the electrical contacts. The latter must indeed be able to extract the photo-generated charge carriers from the PAL, hence the importance of using highly conductive electrodes and of the minimization of the contact resistance at the electrode/PAL interface. Both factors contribute to the reduction of the series resistance in the OPV stack. This reduction is important for device improvement, especially for devices with large scale-up areas and/or exposed to high light intensities [156].

The choice of the electrode materials is determined by their work function (W_f), the cell layout and the energy band diagrams of the PAL active materials. In order to get maximum V_{oc}, the W_f of the metal electrode needs to have an equal or a lower W_f value than the energy value of the LUMO of the electron acceptor compound of the PAL for regular cells, or to have an equal or higher W_f value than the HOMO of the electron donor in the case of inverted cells. It has been demonstrated that a variation of the metal electrode leads to a universal behavior of the photocurrent when scaled against the effective voltage across the device [58]. A common way to tune the metal W_f in function of the requirements of the cell stacking can be achieved by using alloys [157,158].

Depending on the material(s) considered, several degradation mechanisms can occur. The degradation can be localized in the electrode layer itself or at the electrode/PAL interface. In this last case, the degradation mechanisms generally lead to a decrease of the interface quality between the PAL and the electrode (which is equivalent to a loss in active electrode area), therefore leading to a reduction of the charge transfer and extraction. This reduction of electrode/PAL interface can be due to physical loss of contact between the two layers due to delamination [159], creation of voids (for instance when ITO etching takes place [160]) or to the formation of electrically insulating patches at the interface [159–163] due to change of chemical reactions at the surface of the metal electrodes.

In this section of the article, degradation mechanisms of each type of electrodes, either metal- or metal oxide-based will be presented, as well as strategies currently developed to minimize them.

3.3.1. Metal electrodes

Metals are widely used as electrodes for OPV due to the possibility to deposit them as electrically conductive films with thicknesses in the order of 100 nm. Although metal films thinner than 100 nm generally display a higher resistivity than the corresponding bulk materials, the levels achieved are still sufficient for OPV applications. This decreased conductivity of thin films is caused by surface scattering, grain boundary or impurities scattering, as well as by morphological defects [164,165].

Metals typically used for the low W_f electrode (in the case of the regular stack, in which the metal electrode is the electron collecting electrode) are calcium and/or aluminum [160]. Degradation of these negative electrodes is mainly caused by metal oxidation (Ca being more reactive towards oxygen than Al in this respect [159,160]). It is generally agreed that oxygen and water can diffuse through the metal boundary and pinholes to cause modification of the inner interface of the electrode. As a result, a chemical reaction with O_2 and H_2O takes place [166,167]. The latter leads to the formation of voids or insulating patches (inducing a reduction of electrode/PAL charge transfer), which can be coupled to mechanical disintegration and ultimately to delamination when longer exposure times (in the order of months) and/or mechanical stresses are considered [159,160,162,163,168,169]. Alternatively, insulating patches can also be caused by other chemical reactions between the PAL and the metal electrode. As an example, Krebs and his coworkers reported that radical species formed in the PAL may react with the Al electrode, leading to a gradual deterioration of the PAL/electrode interface quality [170]. In both cases, degradation leads to the reduction of the contact area of the metal/PAL interface, which can be evidenced by an increase of the series resistance and thus a decrease of *FF*.

Changes of energy levels, i.e. of the W_f value, may alter the ability of the electrode to fulfil its role as a charge extractor. As an example, an increase of the W_f value of Ag electrodes due to silver oxide formation has been reported to lead to deterioration of the electrode's ability to extract electrons because of level mismatch with the HOMO of the electron donor [160,171]. Nevertheless, this effect is not necessary detrimental to the overall performance of the whole cell: in case Ag is used as top electrode in an inverted cell structure, that is to say as hole collector, formation of silver oxide is actually advantageous.

Regarding high W_f metal electrode choice, silver is often privileged, due to its high stability towards oxidation, as well as because it can be processed by vacuum-free solution-based methods such as printing or spraying, which are compatible with roll-to-roll production [172,173].

However, there are some concerns that, in the case of the inverted cell structure, similarly to what has already been observed in OLED devices [174–176], Ag migration through the PAL and other layers may take place. In OLEDs, this metal migration is due to oxidation by electrolysis of the electrode and application of a D–C field accelerates this diffusion. Suh et al. observed Ag diffusion from the top electrode to the interface between PEDOT:PSS and the PAL of inverted OPV cells stored at indoor ambient conditions. By TEM, they imaged silver particles located at the interface of the PAL and of the buffer layer, which did not seem to migrate through the PAL. Light appeared to accelerate the Ag particle formation and growth, and thus the deterioration of the OPV cell electrical characteristics [177]. Ultimately, it is feared that Ag diffusion might create shorting problems when the migrated metal reaches and contacts the opposite electrode. Considering the lack of experimental data and study dealing with this phenomenon, it is still difficult to assert to which extent this metal migration could jeopardize the OPV inverted cell lifetime.

3.3.2. TCO-based electrodes

The second type of widely used electrodes are metal oxide-based electrodes. Transparent Conductive Oxide

films (TCO) are typically semiconductors that can display metal-like characteristics upon doping. They possess band-gaps larger than 3 eV and are transparent for wavelengths higher than 400 nm [178]. These properties make them suitable to be used as transparent electrodes in OPV devices. The most widely used are indium-tin oxide (ITO, In_2O_3:Sn) and fluorine-doped tin-oxide (FTO, SnO_2:F). Tuning of their properties can be achieved by adjustment of the film deposition procedure and of the component proportions in binary and/or ternary compound alloys [179,180]. Unluckily, TCO film surfaces are polar and hydrophilic, which is unfavorable towards wetting and thus adhesion of the apolar organic PAL while the latter is directly deposited on top of the TCO [181]. Consequently, poor adhesion between the two layers favours delamination and high series resistance.

Strategies to improve the wetting between the TCO and the PAL, and thus the electrode/PAL interface stability, include TCO surface modifications such as plasma treatment or covalent attachment of polar groups [182], as well as the utilization of a buffer layer.

Common suitable buffer layers between the TCO electrode and the PAL in OPV are poly(ethylene dioxythiophene) doped with polystyrene sulfonic acid (PEDOT:PSS) [183,184], as well as transition metal oxide such as V_2O_5 and MoO_3 [185]. In addition to enhancing the OPV efficiency (notably by reducing leakage currents and improving the contact between the TCO and PAL), buffer layers can contribute to preventing undesirable chemical reaction or dipole formation at the TCO:PAL interface.

This may contribute to an increase of the lifetime of the device in two cases:

(I) if no reaction occurs leading to a decrease of the overall quality of the charge transport between the TCO and the buffer layer or the PAL and the buffer layer,
(II) in case that such a reaction occurs, if the kinetics of this reaction are much slower than the reaction that may occur between the TCO and the PAL in the absence of buffer layer.

One of the most largely documented TCO-buffer couple is PEDOT:PSS and ITO. Due to its excellent thermal stability, transparency, conductivity and its ease-of-processing, PEDOT:PSS is widely used as a buffer layer between the ITO and the PAL of OPV devices. It has been shown that using PEDOT:PSS was beneficial towards OPV overall performance. Firstly, due to its higher W_f than ITO, its incorporation in between ITO and the PAL can lead to increased V_{oc} and power conversion efficiency as compared to devices without PEDOT [170,186,187]. In addition, the possibility to relatively easily tune the W_f of this materials by adding e.g. NaOH or CsOH [188], oxidizing or reducing agents [189], as well as by applying an electrochemical treatment [190] to the dispersion, makes it very attractive. Secondly, using a PEDOT:PSS buffer layer can be part of a strategy aiming at improving the wettability of the metal oxide to the non polar organic PAL, therefore decreasing the risk of delamination and high series resistance [181]. Thirdly, since it covers ITO rough surface, it can act as a planarization layer that reduces microscopic shorts formation [191]. It was indeed shown that an uneven electrode/PAL interface is undesirable from the point of view of both OPV efficiency and stability. Cells with rough PAL/electrode interface exhibit small shunt resistance, inducing hence high leakage current and thus small V_{oc} and *FF* values [192]. PEDOT:PSS can also prevent PAL component oxidation by hindering oxygen diffusion out of the ITO electrode [193].

However, PEDOT:PSS has already been reported to be at the origin of OPV cell degradation, mainly due to its hygroscopic nature [194]. First, water absorption by PEDOT:PSS can lead to formation of spatially inhomogeneously distributed insulating patches at the PAL/PEDOT:PSS interface, which most probably result from the reaction of the acidic species PSS with water. This leads to a decrease of the active PAL:electrode area and thus a proportional decrease in the photocurrent and *FF* of the device [161]. Secondly, it has been shown by TOF-SIMs and Rutherford backscattering spectrometry that the ITO/PEDOT:PSS interface can be unstable. The acidic nature of PSS triggers ITO etching and the liberation of indium ions which may diffuse through the PEDOT:PSS and the PAL [193,195]. In all cases, degradation of the quality and/or surface of the ITO/PEDOT:PSS interface, i.e. of the electrode, can significantly affect the overall performance of the cell over time. Although element migration resulting from ITO etching has been monitored, it remains unclear whether the etched species can effectively react with compounds present in other layers of the stacking and negatively affect OPV cell properties [193,195,196].

Additionally, ITO is a brittle material, meaning that it is vulnerable to cracks upon bending of the flexible substrate onto which it is deposited. Crack formation and its propagation in the ITO layer hinders charge transport and increases the sheet resistivity [197]. These poor mechanical properties, combined with high ITO purchase and deposition costs [198] and poor ITO/PEDOT:PSS interface stability have encouraged the search for (i) alternative preconditioning of the ITO surface prior to organic layer deposition (by passivation by plasma treatment of different gases [199], annealing at high temperature to prevent oxygen contamination [200], or chemisorption of small molecules at the ITO surface [182], among other strategies), (ii) use of neutral grades of PEDOT:PSS [201] or (iii) complete replacement of the ITO electrode by alternative transparent materials such as highly conductive conjugated polymers like poly(aniline) (PANI) [202,203] or PEDOT:PSS with enhanced conductivity (which can be achieved for instance by the addition of a high boiling point solvent such as dimethylsulfoxide DMSO [204]). The latter can only be used as top or bottom electrode in combination with metal (Au or Ag) current collecting grids to enhance the conductivity and charge collection. This combination is very beneficial for processing of large area cells, without substantial performance losses. Fig. 4, shows an example of such a cell [205–214]. Another possible alternative method may be to substitute ITO by a semi-transparent (non-patterned) metal layer [215]. Many efforts are also devoted to the development of transparent electrodes based on electrically conductive particles, such as carbon nanotubes [197,216]

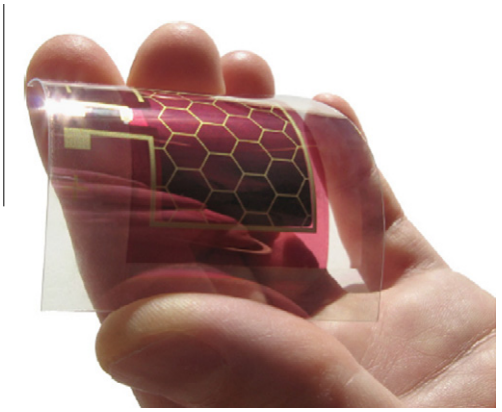

Fig. 4. Picture of a flexible, ITO-free device, with the following stacking: Plastic substrate/barrier film/printed silver current-collecting grid/PEDOT:PSS/photoactive layer/LiF/Al/barrier film. (Reproduced with permission of Ref. [211] Copyright 2010 Elsevier Ltd).

and graphene [217], used as such in thin films or blended in a polymer matrix.

3.3.3. Prevention of electrode degradation

Ways to prevent OPV electrode degradation are various. The most straightforward method consists of preventing the metal electrode to get into contact with degradation triggers, mainly oxygen and water. The latter can be introduced into the device during manufacturing and deposition of the successive layers of the stacking in an inert and moisture-free environment. They can also diffuse from the outside environment to the inner layers of the finished OPV cells.

Regarding the first point, minimizing exposure towards oxygen and water during processing should in principle contribute considerably to an increased lifetime of OPV cells. This can be achieved by working in a moisture-free, inert atmosphere. Nevertheless, this option is not really suitable for upscaling in an industrial environment as it will add to the production costs. If this is not possible, reducing the exposure time of the layer(s) to oxygen/water-containing atmosphere, by for example using a high processing speed, could be an option. Another possibility consists of refreshing/preconditioning the already deposited layer prior to deposition of the subsequent layer (for example, by shortly heating PEDOT:PSS in order to remove water) [204].

Prevention of water and oxygen ingress is generally achieved by the use of a barrier which impedes oxygen and water ingress into the OPV stack, optionally combined with plastic films containing UV filters. This point will be developed into more detail in the following part of the paper.

Tuning the device layout so that materials which are less sensitive to degradation can be employed is also possible. This is the main reason why "inverted" cells, with high work function top electrodes like e.g. Ag or Au, are more stable than "regular" devices, in which often low work function metals like Al and Ca are used as top electrode [160,172].

The use of buffer layers, as already described in the previous paragraph for the particular case of ITO/PEDOT:PSS is also a suitable and widely spread solution. In the particular case of Al used as metal electrode, it was found that sandwiching a thin LiF buffer layer of the order of 1 nm thickness between the Al electrode and the PAL contributes to an enhancement of the performance of the devices (as evidenced by an increased *FF* and J_{sc}). The exact underlying reasons at the origin of these effects are still under debate [13,218]. It has notably been mentioned that it could be due to the formation of a dipole moment at the interface of the OPV cell, leading to a decrease of the electrode work function and an improvement of the ohmic contact [218]. The effect of LiF on OPV cell stability remains unclear. Some researchers found that the LiF buffer layer contributed to an enhancement of the OPV cell stability, possibly because of an inhibition of Al oxidation and thus electrode degradation [162,166]. It was also reported that using a thin layer (on the nm scale) of either lithium benzoate (C_6H_5COOLi) [219] or Cs_2CO_3 [220], also contributes to an improvement of OPV cell performance (resp. lifetime). The origin could be an enhanced ohmic contact (resp. possibly hindrance of Al oxide formation and/or water and oxygen ingress). On the other hand, other researchers did not observe any significant improvement of OPV lifetime due to the addition of a LiF buffer layer [170]. These observations suggest that these effects might be more connected to the OPV layer deposition conditions. To the best of the authors' knowledge, degradation of most buffer layers other than PEDOT:PSS has not been documented in literature yet.

3.4. Barrier and substrate

Next to the work at the materials level (e.g. careful choice, processing and combination of materials) complementary strategies developed to increase the OPV lifetime focus on the development of barrier films. This research effort is more particularly aimed at hindering degradation triggers such as water and oxygen to "reach" the OPV cells component. In other words, this strategy consists of reducing as much as possible the causes of extrinsic degradation. The latter appears indeed to be one of the most critical parameter in preserving device performance during lifetime tests [198].

Since OPV electrodes alone are not sufficient to suppress, significantly reduce or slow down moisture and water ingress [85], the use of extra layers, so-called barrier layers, to encapsulate the system is required. It is not very well-defined what the exact requirements for the barrier properties should be. It is generally assumed to be comparable to the gas permeation rates required for OLED, i.e. in the range of $5\ 10^{-5}$–10^{-6} g m^{-2} day^{-1} (resp. 10^{-3}–10^{-5} cm^3 m^{-2} day^{-1} atm^{-1}) for moisture (resp. oxygen) ingress [74,221], although some studies point out that OPV barrier requirements might be less demanding to achieve manufacturing of OPV with significant lifetimes, i.e. in the order of several years [222–224].

From Fig. 5, it can be seen that transparent and flexible barrier films like those used to encapsulate OLEDs [225,226] can cut oxygen and water ingress, and therefore

prevent degradation of a flexible plastic OPV cell as effectively as an aluminum lid containing a getter and glued on a glass substrate. For two series of OPV cells prepared in the same way, no significant degradation difference could be evidenced for both types of substrate and encapsulation after 1000 h of testing at 1 sun illumination and 45 °C. The average degradation in performance was a decrease of about 5–8% in efficiency after 1000 h of exposure.

Both water and oxygen are degradation triggers. However, the relative importance of the action of each of them is connected to the degradation effectively taking place in a given sample, meaning that it is indirectly strongly connected to the OPV cell layout, material selection and processing conditions [172,227]. In an attempt to isolate specific degradation triggers of inverted and regular OPV architectures, Krebs and his co-workers [172] recorded the *I–V* characteristics over time of inverted and regular OPV cells (see Fig. 6) placed in an atmosphere with controlled water and/or oxygen contents. From this study, it was possible to determine that inverted (resp. regular) cells were more prone to quickly degrade (that is to say that non-encapsulated cells were not delivering any current anymore within a few tens of hours) while put in contact with oxygen (resp. water). These results were in line with those of Cros et al. [223]. These researchers reported that, in order to reach half of the initial efficiency value of a given OPV device, 60 times more water (diffusing through the barrier film) was needed for inverted solar cells than for regular cells. In other words, when tested in the same conditions of relative humidity, inverted cells require more time to degrade and hence are more stable than cells with a regular architecture.

These findings clearly point out that degradation paths differ between the two cell architectures. In Krebs' article, the two types of cells, inverted and regular, possessed the same type of photoactive layer, which had been processed in an identical way for both cell architectures. If applicable, the cells had also been encapsulated in the same way, with the same barrier film. On the other hand, the electrodes were different between the two cell architectures, which means that degradation was likely to be located at the level of the electrode stack (i.e. electrode and buffer layer) and/or PAL/electrode interface.

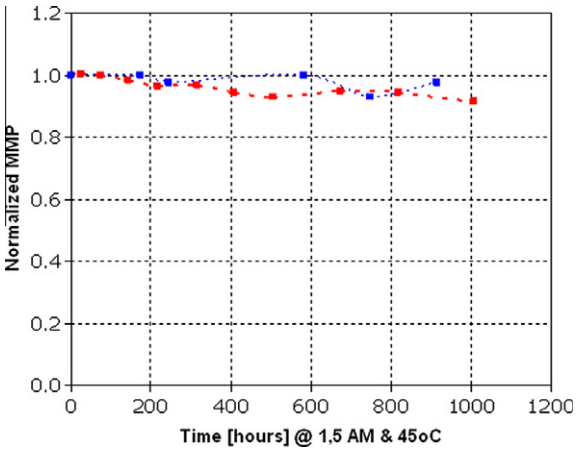

Fig. 5. Normalized MPP plotted in function of time of 2 2 cm^2 cells with the same layer processing and stacking (printed silver current collecting grid/ PEDOT:PSS/PAL/LiF/Al) but different encapsulation methods: *Blue curve:* OPV device processed on top of a multi-layer barrier stack on PEN and "closed" with a thin film barrier encapsulation and *Red curve:* OPV device processed on top of a glass substrate and "closed" with an aluminum lid containing a getter and an epoxy adhesive.

For regular devices, degradation often occurs due to oxidation of the metal top electrodes which hinders charge transfer from the PAL to the electrode (leading mainly to a decrease of *FF* and J_{sc} [160]). On the other hand, degradation of the bulk material seemed to be the dominant reason of degradation of the inverted cell performances. After a detailed study of the degradation of inverted cells, Norrman et al. came to the conclusion that the major failure mechanism was related to PEDOT:PSS phase separation and the subsequent deterioration of the PEDOT:PSS/PAL interface [227].

In order to fulfil their role, barrier films must offer properties which are comparable to those of glass, such as transparency, dimensional and thermal stability, chemical resistance, as well as low moisture and oxygen permeation. No polymer as such can combine all these properties. To give an estimate, a simple polymer film like the one used to package e.g. food or drugs do not perform better than 10^{-2} g m^{-2} day^{-1} (water vapor transport rate (WVTR) value).

In theory, a single perfect silica layer of a few nm thickness should be impermeable to moisture and oxygen. In practice, inorganic thin film layers always have nano- to micro-sized defects called pinholes [228]. The latter originate from the deposition process used and/or from the roughness of the underlying substrate onto which the layer is deposited. These pinholes offer permeation paths for moisture and oxygen, therefore limiting the barrier performance. Successive deposition of inorganic films on top of each other does not usually significantly improve the barrier performance due to the propagation of the defects through the layers during film growth [228].

The solution consists of using barrier films made of alternating organic–inorganic thin layers [228–232]. The inorganic layer plays the role of "barrier" which hinders water and oxygen penetration, while the organic layer contributes to the reduction of the number of pinholes because it simultaneously smoothens the coated surface, reduces mechanical damage, as well as increases the thermal stability of the inorganic layer. In other words, this multilayered geometry leads to a dramatic reduction of the water and oxygen ingress rate by several orders of magnitude, by providing a longer, tortuous diffusion path [233]. Furthermore, each layer contributes to the mechanical behavior of the whole structure [234,235].

Flexible OPVs are typically prepared on flexible substrates like polyethylene naphthalate (PEN) or polyethylene terephthalate (PET) films. Most of the time, the barrier film is present on both sides of the OPV cell. It can be laminated onto the substrate film (hence the use of adhesives is needed) or directly deposited layer by layer on the system requiring protection. Special care should be taken not to entrap water or oxygen during encapsulation and/or to remove any residual moisture and oxygen once

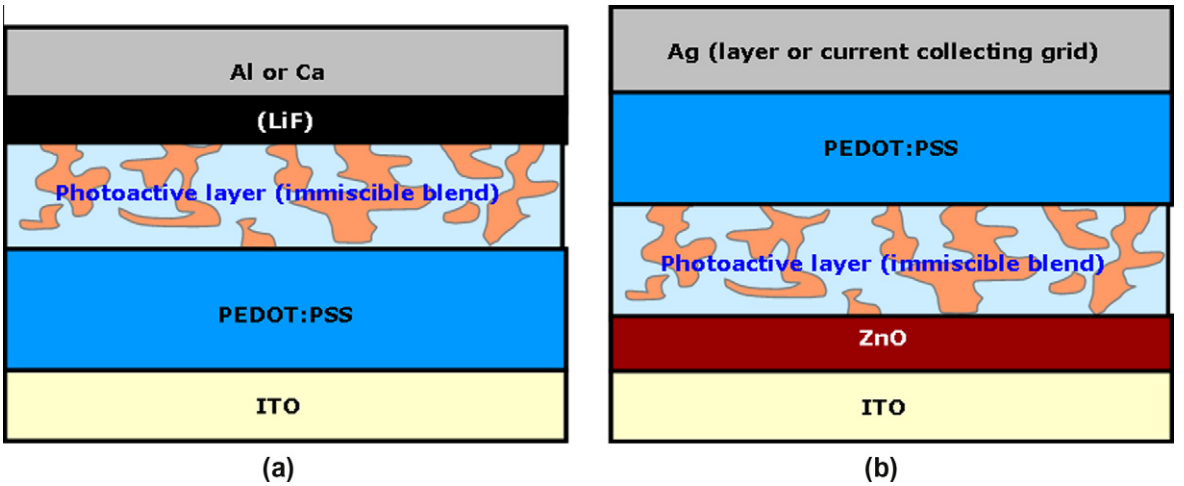

Fig. 6. Schematic representation of an OPV bulk-heterojunction cell structure: (a) regular and (b) inverted architecture. These cells may be sandwiched between two barrier layers.

the cell has been encapsulated. These two compounds can be adsorbed on the surface of the cell, or even be present in the bulk of the materials (e.g. in the PAL), and therefore trigger fast initial decay of the cell [221].

Degradation of the substrate and of the barrier can occur at different levels:

(i) at the edges, when adhesives are used. For example, degradation of the adhesive used to seal the module may induce the release of some by-products which can induce the decay of the cell. One way to minimize these effects consists of adding a moisture and oxygen getter material such as calcium oxide [236],
(ii) in the polymeric layers,
(iii) at the level of the inorganic layers.

Independently of the presence of the inorganic layers, polymeric materials age in presence of triggers such as light, water or mechanical stress. The degradation mechanisms listed in the present paragraph are common to most polymeric materials and can thus occur at the level of the alternating organic layer of the barrier film or the base substrate. In addition to fatigue that occurs when the materials are put under mechanical stress, non-cross-linked polymers can become brittle over time because of local reorganization/orientation of the chains, which contributes to an increase of the yield stress of the materials and enhances its brittleness [237]. This effect is strengthened by exposure to UV light. The latter promotes chain scission which results in embrittlement and modification of the optical properties of the polymer (i.e. decrease of transparency due to chemical degradation (yellowing)), as well as an increase of light scattering due to physical reorganization of the polymer chains leading to formation of larger crystals; in both cases (chemical degradation and larger crystal formation) photon absorption of the polymeric materials is decreased at the macroscopic level [235,238,239]. Studies dealing with this matter were done on commercial polymer films alone. In particular, no study of the changes in optical properties of a barrier film (multilayered system made of polymer layers alternating with inorganic thin layers) considered as a whole has been reported so far [74]. These effects can be significantly cut by using additives such as UV absorbers (UVA) [240] or toughenersers [235] during manufacturing, or by using copolymers with elastomeric chains can be carried out in order to lower the stiffness of the resulting materials. The chains form 10–20 μm-large separate phases in the solid so that crazes form at their surfaces when the material is strained.

Mechanical stress constitutes the main cause of degradation of the inorganic layers of the barrier film which, contrary to organic materials, are very stable towards light. Mechanical integrity of the multilayered structure is difficult to maintain as these systems are made of stacks of layers possessing different thicknesses, different mechanical properties (notably the elastic modulus) and different thermal expansion coefficients. As a consequence of these dissimilarities and of the high deposition temperatures during manufacturing, residual strains and stresses remain in the layered barrier. Under thermal and/or mechanical stresses (such as compressive strain or bending) and/or residual strain, defects present in the inorganic layer can lead to cohesive failure modes (i.e. cracks) whereas insufficient inter-layer adhesion can result in adhesive failure modes, i.e. buckling and even cracks and/or delamination [234]. In addition to the loss of mechanical properties, failures of the inorganic layers in the multilayered stack also degrade barrier properties (such as water vapor transmission, see Fig. 7) therefore promoting extrinsic degradation. In the worst case, cracks can form at a certain level and propagate through the whole OPV stacking [207,241].

Levels of degradation of the multilayered barrier system can be lowered by improving the processing conditions and/or the material choice in terms of properties and compatibility in order to minimize residual strain and to enhance the level of adhesion between layers of the stack (which may necessitate surface treatment prior to

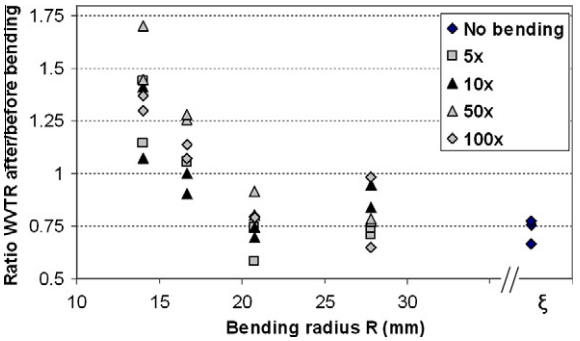

Fig. 7. WVRT ratio after/before bending of a barrier film made of an alternating stacking of SiN and organic layers plotted in function of the bending radius *R*. The initial WVTR of the barrier before bending was 8 10^{-5} g m^{-2} day^{-1} at 20 °C and 50% relative humidity (RH). Significant degradation of the barrier properties of the samples was only observed for bending radii lower than a critical radius of 20 mm. The latter is small enough to enable roll-to-roll processing among others. (Figure adapted from Ref. [225]).

additional layer deposition or use of an intermediate layer), by using thin organic layers. As an example, Abdallah showed that the presence of water in the polymeric layers of the barrier (an aromatic polyester) is detrimental to SiN_x adhesion. Therefore, moisture introduction to the interface during processing must be avoided [234].

3.5. OPV Module degradation

In addition to all the degradation mechanisms that were previously listed, "electrical stress" at the level of the individual or interconnected cells can also lead to significant degradation of PV devices.

For most applications, OPV modules must deliver a voltage which is generally higher than that provided by one individual cell. That is why individual cells are interconnected in series.

Most OPV modules described in literature are monolithically integrated. They usually consist of stripes of the different materials which are stacked on top of each other to form individual cells. In order to allow connection of the top electrode to the bottom electrode of the neighboring cell, each stripe is shifted in comparison with the underlying layer, see Fig. 8.

This module geometry is mainly dictated by the use of ITO as bottom electrode which possesses a relatively high sheet resistance. ITO on glass usually displays sheet resistance values of 10–15 Ohm/Sq, whereas values of 50–70 Ohm/Sq for ITO on foil are more typical [242]. The latter fixes boundaries to the width of each stripe, which is typically the order of 1 cm or smaller for ITO on plastic substrates [242]. The reason behind this difference in sheet resistance is the limited annealing temperature (130–150 °C) that can be applied in case a plastic foil is used as substrate for ITO. Moreover, due to the limitations in annealing temperature for ITO on foil, the ITO surface also has a much higher roughness compared to ITO on glass. This roughness (and spikes) increases the chance of hot spots and short circuits to occur (see Section 3.5.1) and can hence be an additional cause for the faster degradation of OPV (and OLED) [243]. In other words, the use of ITO on foil severely narrows the module processing window in terms of cell and module geometries and lifetime.

Additionally, if only additive solution processing is used, a shift of the position of each individual stripe in comparison from the underling stripe to allow monolithic inter-cell connection is needed. Depending on the ink properties, individual layer shifts of 1–2 mm are often required because capillary forces dominate on this scale and cannot be controlled directly. This leads to considerable aperture losses. As a result, only a part of the surface of a given module, which is of the order of 50–75%, [198,244,245] is effectively contributing to electricity production.

On the other hand, this module geometry (stripes) has the advantage of being relatively easy to pattern, therefore allowing the use of coating and printing techniques during manufacturing. The development of ITO-free cells and modules may lead to alternative ways of serially contacting OPV cells within a module in the near future, which might exhibit lower aperture losses but simultaneously different and/or additional degradation paths.

Interconnected cells may experience specific degradations which might not occur in individual solar cells, as will be explained in the following section.

3.5.1. Hot spots

Shading failure is commonly observed in all PV technologies. It occurs when part of or whole individual cell(s) of the module in operation are shaded. Since in a shaded cell less current is generated the current matching of cells connected in series will lead to a strong decrease of the overall module current. This can lead to two types of failures, one reversible (type I) and one irreversible (type II), depending on the characteristics of the cells and of the module. If the cell possesses a good dark rectification and a high shunt resistance, the photovoltaic power of the non-shaded part of the module is dissipated across the shunt resistance, the current cannot flow through the shaded cell and the whole module stops operating (failure mode of Type I). On the other hand, the second type of failure mode usually leads to irreversible degradation. If the cell has a low dark rectification and a specifically smaller shunt resistance, photocurrent transport through the shaded cell still takes place. As such, the module delivers a PV power which is equal to the PV power of the module minus the power loss required to drive the shaded cell in reverse bias (necessary to allow the leakage current of the cell to match the current of the partially shaded volume). The shaded cell often behaves like a load that dissipates the excess power generated by the other non-defective cells of the module in the form of heat. In this case, the temperature locally increases, leading to the creation of hot spots, i.e. localized regions in which the operating temperature is higher than the one of the surrounding area. This can induce degradation of the materials of the cell and/or short cuts. The heat generated generally triggers further defect growth and thus degradation, leading to a vicious circle.

Hot spots can also occur at the level of non-interconnected individual cells. For example, a higher local shunt on one side of an OPV cell can lead to higher local current

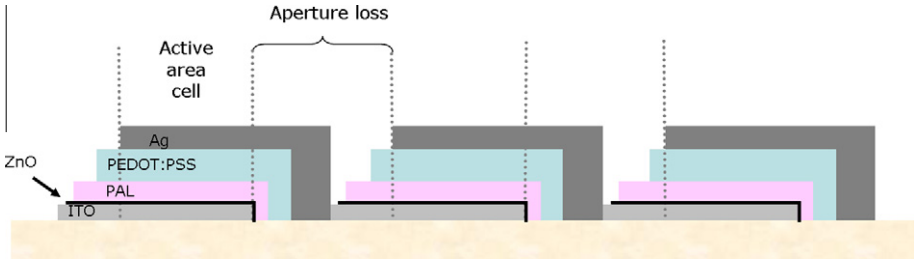

Fig. 8. Drawing of an OPV module (side view) – example of an inverted cell configuration.

through the shunt and to Ohmic leakage [246]. Alternatively, presence of dust particles in the stacking or non-planarity of the organic PAL layer-electrode interface can induce higher local electrical fields, paving the way to the formation of microscopic conduction paths through the organic layer during operation [247]. Similarly, the presence of conductive metal catalyst nanoparticles (such as palladium) formed during polymer synthesis and remaining after purification, may also create small zones within the PAL where conduction preferably takes place. If the particles percolate between the two electrodes, this simply leads to short circuits [248]. Additionally, cracks, cell component degradation, delamination, contact aging, shading, etc. have also been shown to lead to hot spots [249].

Depending on the origin of the hot spots, several actions can be taken in order to protect the cells and modules against them. First of all, opting for a dust-free manufacturing process and storage conditions which minimize risks of cracks (for example by avoiding bending and minimizing handling steps) and dust particle introduction in the cell stacking can already constitute the first steps towards hot spot prevention. Additionally, it has been shown that, after reverse biasing, devices with no or only weak hot spots due to local shunting, experience less degradation under reverse bias. This leads to both a reduced decrease of *FF* and a reduced increase of leakage current, which does not favour the creation of new shunts. Consequently, it can be assumed that cells with higher quality interfaces and bulk materials (e.g. thermally stable materials) will also be more resistant towards hot spots formation [250].

In the more specific case of hot spots occurring because of module shading, one may think of designing modules in which the cells possess specific shapes (concentric rings for example) which might lower the possibility of shading complete cells during operation, an thus minimize the risk of power output losses [251]. Steim et al. showed that another more universally applicable solution is to connect an organic bypass diode, with reverse polarity, in parallel to a group of solar cells in the module [246]. Under shading, the diode forms an alternative current path for the module photocurrent when it opens up. Consequently the voltage drop experienced at the module level is limited to the voltage required to open the bypass diode. Interestingly, Steim and his coworkers show that using an organic bypass diode is advantageous as it also act as an inorganic bypass diode with comparable characteristics. Moreover, a "pick-and-pass" process is no longer needed to integrate it in a (flexible) OPV module as it can be manufactured at the same time as the module with reduced additional processing steps.

3.5.2. Interconnections

Considering the typical architecture of a module, see Fig. 8, degradation processes of inter-cell connections (direct anode–cathode contact) are very likely to be of the same nature as the electrode degradations previously described in more detail in Section 3.3.

Degradation of the connection between the organic module and the "outside world" has currently not been extensively studied yet, mainly due to the novelty of the technology. Most systems studied in literature are individual cells or modules without 'special' interconnects. Commercial devices, which possess this type of connections, have not been described in detail either.

Similarly to other thin film PV technologies, the electrical connection between the module and the "outside world", i.e. consumer goods, electrical grid, etc., is likely to be achieved by soldered joins (for example made of a flat copper ribbon as described in Ref. [198]). As a result, degradation due to corrosion and fatigue of solder bond may take place. As shown by King and Dunlop for crystalline silicon modules, a.o., corrosion of the interconnect, as well as presence of particles (due to contamination from the environment) may induce shunts, which lead to series resistance increase and output power decrease, as well as to safety issues [249,252]. Soldered joins can deform or creep as a result of mechanical cycling, as was already evidenced for crystalline silicon solar modules which had experienced field temperature cycling (mainly caused by the day–night alternation during outdoor tests). Thermal cycling submits the soldered joints to mechanical shear stress because of discrepancies in expansion coefficients of the different materials [253]. Additionally, segregation of metals of soldered alloys, such as SnPb, leading to coarsening and large metal grain formation, has also been reported to seriously jeopardize the mechanical integrity of the joints. The latter results in increased series resistance and output power loss, so, in other words, to shorter module lifetimes.

Flexible (O)PV modules are meant to withstand (repeated) bending with limited power loss and/or permanent deformation. The requirement in term of resistance towards mechanical stress is strongly connected to the end application of the marketable product considered: relatively small items aimed at customer applications must be able to bend many times with a relatively small radius

whereas larger panels to be placed on roofs will only be bended a few times and over long period of times, i.e. during manufacturing, storage, transportation and installation. It may even be required to be able to walk on the panels. It has already been reported that inorganic PV thin films exposed to tensile and compressive stress due e.g. to bending or to thermal cycling (which induces dilatation of the sample layers which possess various dilatation coefficients) experienced increased series resistance, notably due to cracks [254], as well as to layer delamination [255]. Considering the similarity in term of sample structure, (encapsulated) OPV modules are extremely likely to be sensitive towards the same type of deterioration as PV thin film modules of other technologies, as already foreseen in previously published works dealing with the study of OPV-related samples [207,225,234,241].

Degradation by mechanical bending can be reduced by proper handling (e.g. by preventing users from excessively bending the OPV modules [244]), improvement of the inter-layer and joint adhesion, and, as much as possible, by selecting stable alloys and by preferably using materials with matching dilatation coefficients.

4. Lifetime and accelerated tests

Nowadays, most (inorganic) PV manufacturers of solar modules are able to guarantee a minimum performance of their products for 20 years and more. This typically means that their products will perform to e.g. at least 80% over the whole period covered by the warranty. PV desirable module lifetime is usually in the order of years (20–30 years for outdoor utilization). Normal lifetime testing implies analyzing time-to-failure data of the system, obtained in normal operating conditions in order to quantify the lifetime characteristics. Considering the time required for testing (on the order of at least a few decades), as well as the complexity of selectively testing each components of an integrated product, accelerated lifetime tests are widely used. These tests consist of increasing the stress applied to (O)PV devices compared to regular use conditions. In other words, they constitute an attempt to artificially shorten the life time of the device and to therefore find out how a given material, component or integrated product reacts in an acceptable time frame. There are two ways to achieve acceleration of the degradation: stress acceleration (e.g. increase of environmental stress factors) and time compression. In the first case, relevant parameters to take into account are logically the degradation triggers, i.e. light, temperature, moisture, electrical stresses, etc. Time compression is usually achieved by rapidly cycling test parameters. The main difficulty in designing accelerated tests is to keep the conditions relevant and realistic in order to avoid distortion of the degradation mechanisms and failure modes evidenced. Due to the difference of time scale between the accelerated test and the 'real' lifetime test, checking the linear dependence (or degree of correlation) between these two tests is a way to assert the validity of a given accelerated test [256].

For the time being, no general and standardized definition of lifetime for OPV cells has been adopted yet, which constitutes a potential source of misunderstanding. In addition, no set of standard lifetime tests especially designed for OPV cell and/or modules exist, making it hard to compare results reported in literature, conferences and/or in OPV manufacturer brochures. Even if OPV technology has not reached any large-scale commercialization yet, it appears crucial to establish lifetime test standards in order to allow unbiased comparison of results obtained by different research groups and companies, among others, as well as to reduce data spread due to the diversity of measurement procedures and equipment from one laboratory to the other.

Part of these test standards is likely to be different from the existing standards defined for more mature, non-flexible, inorganic technologies. Flexible OPV specimens indeed possess a few specificities that may render the direct use of some widely applied standardized tests irrelevant. Firstly, (O)PV modules can be seen as "plastic-related" products, for which tests have already been designed and implemented in industries such as coatings, building, automotive, packaging and cabling, a.o. and it would certainly be relevant to adapt them to test OPV products. Secondly, photodoping of one or several components of the devices due to uncontrolled exposure to light of the samples prior to measurements may lead to inaccurate or erroneous lifetime determinations [96,257,258]. The significance of this effect is directly related to the choice of the cell architecture and components, and is therefore likely to differ from one type of device to the other. Additionally, samples produced by roll-to-roll can be flexible. As a result, mechanical stress, notably induced by handling the samples during lifetime test measurements, can significantly affect the rate of degradation of the samples [244]. Standardized mechanical tests aiming at characterizing the (loss of) PV performances as a function of time are very likely to be needed in the future in order to monitor OPV module mechanical aging (upon storage on the manufacturing rolls or during use).

The few lifetime tests performed on flexible OPV modules reported in literature were carried out over relatively short time frames (generally a few months). The modules were prepared in different ways, with cells of various architectures, and the lifetime tests performed under various conditions in terms of lighting, relative humidity (RH) values, encapsulation systems, make a direct comparison of the results very difficult, see Table 3.

The so-called International Summit on OPV Stability (ISOS) [259] was initiated in 2008 to establish a set of standardized (accelerated or not) lifetime test procedures in order to homogenize practices and thus to allow direct inter-organization result comparison. The focus of this summit is to yearly gather the OPV international community in order to discuss problems related to organic photovoltaic (OPV) stability, especially those which are the most relevant to measurement practices.

Tests selected by the third edition of ISOS (ISOS-3) in order to test lifetime of OPV modules produced by roll-to-roll at the Risø institute were: shelf life study (samples typically stored in the dark, under controlled or not RH and T), light soaking tests and outdoor testing. Results of these tests are shortly summarized in Table 4.

Table 3
Lifetime studies reported in literature of flexible OPV cells and modules processed on flexible plastic substrates.

Ref.	Device stacking	Experimental conditions of lifetime test carried out/WVTR barrier used	Lifetime measured
[224]	ITO/PEDOT:PSS/P3HT:PCBM/LiF/Al Batch-to-batch processed (doctor blading and spin coating)	Outdoor test/0.03 g m^{-2} day^{-1}*	15% eff. loss after 14 months reported (underestimation in paper due to poor module preconditioning)
[172]	ITO/ZnO/P3HT:PCBM/PEDOT:PSS/Ag Roll-to-roll processed	Controlled atmosphere**/constant illumination/no encapsulation	No significant degradation when stored in dry N_2 – <10% of efficiency loss after 200 h in O_2 – "Death" in less than 10 h in humid N_2
[172]	ITO/ZnO/P3HT:PCBM/PEDOT:PSS/Ag Roll-to-roll processed	Controlled atmosphere**/constant illumination/25 μm thick PET film so WVTR of the order of 0.01 g m^{-2} day^{-1}	No significant performance loss after 200 h in dry and humid N_2 – "Death" of the device after 150 h when storage in air
[242]	ITO/PEDOT:PSS/P3HT:PCBM/Al Batch-to-batch processed (doctor blading)	Shelf life#/storage in dark/<5 10^{-3} g m^{-2} day^{-1}	50% eff. loss after 6000 h storage
[198]	ITO/ZnO/P3HT:PCBM/PEDOT:PSS/Ag Roll-to-roll processed – Assembly of grid-connected modules mounted onto glass	Outdoor tests/various types of barriers used	Best panels retained 80% performance for over one month

* WVTR value measured at 38 °C, with 100% RH.
** For Ref. [172]: dry O_2 and N_2 possess water concentrations <1 ppm/humid N_2 to 90 ± 5% of relative humidity and an oxygen concentration smaller than 1 ppm. $T = 40 \pm 3$ °C.
\# For Ref. [242]: devices stored in dark, at 20–25 °C and 30–35% RH.

Table 4
Summary of lifetime tests carried out on OPV modules produced by roll-to-roll [244]. The cells of the modules possessed the following stacking: ITO/ZnO/P3HT:PCBM/PEDOT:PSS/Ag and were encapsulated with a barrier foil which was delaminated.

Tests carried out	Time	Normalized PCE
Shelf life study (dark under ambient conditions *or* in controlled T/RH chamber)	200 h	95 ± 4.8%
	400 h	89 ± 6.6%
	700 h	76 ± 8.9%
	1000 h	68 ± 13.0%
Light soaking in indoor conditions	T > 65 °C and RH > 60% = >detrimental to module stability Degradation rate strongly connected to the spectrum of the lamp used	
Outdoor studies	200 h	84 ± 6/87 ± 13%
	400 h	66 ± 11/74 ± 18%
In-situ/ex-situ (hence extra handling involved) measurements	700 h	52 ± 9/64 ± 16%
	1000 h	44 ± 9/48 ± 21%

The lessons learnt from this study were numerous and recommendations for relevant measurement conditions could be formulated [244]. Since OPV stability is directly related to the temperature, the RH percentage, the periodicity of handling, as well as the spectral distribution of the light source used (which furthermore may evolve over the time scale of the study due to lamp aging), standardizing (or at least keeping track of) these testing parameters appears crucial. The importance of sample preconditioning at the beginning of the lifetime test, for example by light soaking due to the ZnO buffer layer used in the device tested in the inter-laboratory study [257], was also clearly evidenced.

5. Conclusions

To sum up, the main degradation mechanisms of OPVs are listed below, as well as their implications and triggers:

- chemical degradation or oxidation of the compounds of the photoactive layer (caused by moisture, oxygen and/or light), phase separation of the blend (heat), crack formation (mechanical stress). Chemical degradation of the PAL components and cracks are damaging to charge (hole and electron) transport through the PAL, whereas blend phase separation may lead to a loss of charge separation efficiency,
- chemical reactions leading to degradation and/or oxidation of the electrodes (due to moisture, light and/or heat). These generally lead to degradation of the PAL-electrode interface due to a decrease of the interfacial area because of formation of insulating layers and/or voids. All these changes deteriorate the charge transfer from the PAL to the electrodes. Atoms or molecules resulting from chemical degradation of the electrode can then migrate through the other layers of the OPV cell, which may in some cases be damaging to the performance of the cell,

- regarding the barrier and substrate, the main degradation mechanisms occurring are linked to the polymeric nature of the materials used and can lead to a loss of flexibility (because of an increase of stiffness due to polymer aging accelerated by light, moisture and heat). This can ultimately lead to cracks and/or delamination and/or yellowing of the polymer (caused by light, heat and moisture, and which leads to a decrease of photon absorption),
- at all levels of the stacking, cracks and/or delamination between layers can occur. These phenomena are triggered by mechanical stress,
- aging of polymeric adhesives that may be used in some cases to laminate the barrier film onto the OPV device (common polymer aging amplified by moisture and oxygen). This leads to an increase of side leakage (higher moisture and oxygen permeation),
- finally, electrical stress (in the OPV cell itself or between cells in the case of a module) caused by for instance shading can induce hot spots, which ultimately lead to degradation of the system.

It is important to emphasize that most of the degradation mechanisms reviewed here are common to many organic materials and will take place, regardless of the specificities of the material used. Of course, these degradation mechanisms may differ from one system to another to which extent they occur. Additionally, the exact degradation pathways are likely to differ in the details. Moreover, the kinetics of a given degradation route depends on the degradation mechanism itself, its localization (bulk or interface), the sensitivity of a material to the degradation trigger (in other words: what is the minimum threshold in terms of contact with the degradation trigger which will lead to a measurable impact on the OPV performances?), as well as its degree of exposure (e.g. cell encapsulated or not, stored in the dark or under sun or artificial light), etc.

Decay in *I–V* characteristic values is typically due to the combined effect of sequential and interrelated degradation mechanisms occurring at various paces, at different levels of the OPV cells and modules. As a consequence, it remains difficult to pinpoint which degradation mechanism is significant or predominant at a specific time of the device lifetime. Working with model systems (which may be only parts of a complete device) and the use of complementary characterization techniques is extremely important to trace the origin of OPV degradation.

Materials used to prepare OPV, as well as cell and module designs, are moving targets. As a result, it is difficult to propose a precise description of a standard OPV cell and/or module, making a ranking of degradation mechanisms as a function of occurrence and detection problematic. In particular, the resistance towards degradation constantly improves.

We believe that the OPV PAL chemical and physical (e.g. phase separation) stability, as well as the barrier and substrate properties will remain critical since polymeric materials are known to be less durable materials over periods of time in the order of decades for outdoor applications (tires, car paint, etc.). Interfacial stability remains an issue, although it can be manipulated and improved to a certain extent by careful material selection and combination, by tuning the deposition conditions and the thickness of the different layers, as well as by using different device stacks. In fact, interfacial phenomena may occur subsequently to relatively small/short contacts with degradation triggers, which means that a limited degree of degradation can have a profound impact on the overall performance of the device.

It remains relatively unclear to which extent OPV cells and modules should be resistant towards degradation and which degree of degradation is acceptable to guarantee a specific lifetime. In this respect, note that the notion of lifetime is strongly related to the end application of the product. As an example, a lifetime of a few years with indoor use is acceptable for a cell phone battery charger, whereas a minimum of 20–25 years is expected for outdoor applications. In all cases, for future commercial applications, as well as to allow unbiased comparison of results, efforts of the OPV community to established standardized lifetime definitions and tests are needed.

Acknowledgements

This review was written in the framework of Holst Centre's shared research programs and in collaboration with the Energy Research Centre of the Netherlands (ECN). The authors also would like to thank the HiFlex, geZONd and OzoFab projects for financial support.

References

[1] (www.iea.org).
[2] R.W. Bentley, Energy Policy 30 (2002) 189–205.
[3] R.A. Kerr, Science 318 (2007) 1230.
[4] W.A. Hermann, Energy 31 (2006) 1685.
[5] Statistical Review of World Energy – British Petroleum (July 31, 2006).
[6] (www.iea.org/papers/2010/pv_roadmap.pdf).
[7] N.S. Lewis, MRS Bulletin 32 (2007) 808–820.
[8] (http://www.eia.gov/forecasts/aeo/index.cfm).
[9] J. Kalowekamo, E. Baker, Solar Energy 83 (2009) 1224–1231.
[10] G. Dennler, C.J. Brabec, Socio-economic Impact of Low-Cost PV Technologies, in: C.J. Brabec, V. Dyakonov, U. Scherf (Eds.), Organic Photovoltaics: Materials, Device Physics, and Manufacturing, Wiley VCH Verlag GmbH & Co., Weinheim, 2008.
[11] J. Schmidtke, Optics Express 18 (2010) A477–A486.
[12] C.J. Brabec, J.A. Hauch, P. Schilinsky, C. Waldauf, MRS Bulletin 30 (2005) 50–52.
[13] C.J. Brabec, Solar Energy Materials and Solar Cells 83 (2004) 273–292.
[14] F.C. Krebs, Refocus 6 (2005) 38–39.
[15] M.A. Green, K. Emery, Y. Hishikawa, W. Warta, Progress in Photovoltaics: Research and Application 17 (2009) 320.
[16] M.C. Scharber, D. Mühlbacher, M. Koppe, P. Denk, C. Waldauf, A.J. Heeger, C.J. Brabec, Advanced Materials 18 (2006) 789–794.
[17] L.J.A. Koster, V.D. Mihailetchi, P.W.M. Blom, Applied Physics Letters 88 (2006) 093511.
[18] A.E. Becquerel, Compt. Rend. Acad. Sci. 9 (1839) 561.
[19] A.E. Becquerel, Compt. Rend. Acad. Sci. 9 (1839) 145.
[20] W. Smith, Nature 7 (1873) 303.
[21] W.G. Adams, R.E. Day, Proceedings of the Royal Society of London Series 25 (1876) 113.
[22] A. Pochettino, Acad. Lincei Rend. 15 (1906) 355.
[23] M. Volmer, Annals of Physics 40 (1913) 775.
[24] in: www.chemheritage.org (article over Leo Hendrik Baekeland).
[25] F.K. Hansen, Historic overview, in: A.M. van Herk (Ed.), Chemistry and Technology of Emulsion Polymerization, Blackwell Publishing Ltd, Oxford, UK, 2005.
[26] R. McNeill, R. Siudak, J.H. Wardlaw, D.E. Weiss, Australian Journal of Chemistry 16 (1963) 1076–1089.

[27] B.A. Bolto, D.E. Weiss, Australian Journal of Chemistry 16 (1963) 1076–1089.
[28] B.A. Bolto, R. McNeill, D.E. Weiss, Electronic Conduction in Polymers III, Electronic Properties of Polypyrrole 16 (1963) 1090–1103.
[29] J. McGinness, P. Corry, P. Proctor, Science 183 (1974) 853–855.
[30] T. Ito, H. Shirakawa, S. Ikeda, Journal of Polymer Science – Polymer Chemistry Edition 12 (1974) 11.
[31] C.K. Chiang, Y.W. Park, A.J. Heeger, H. Shirakawa, E.J. Louis, A.G. MacDiarmid, Physical Review Letters 39 (1977) 1098.
[32] H.E. Kiess, Conjugated Conducting Polymers, Springer-Verlag, Berlin Heidelberg, 1992.
[33] K.M. Coakley, M.D. McGehee, Chemistry of Materials 16 (2004) 4533–4542.
[34] R.H. Bube, Photoelectronic Properties of Semiconductors Cambridge University Press, Cambridge University Press, Cambridge, UK, 1992.
[35] I.G. Hill, A. Kahn, Z.G. Soos, R.A. Pascal Jr, Chemical Physics Letters 327 (2000) 181–188.
[36] S.F. Alvarado, P.F. Seidler, D.G. Lidzey, D.D.C. Bradley, Physical Review Letters 81 (1998) 1082–1085.
[37] M. Knupfer, J. Fink, E. Zojer, G. Leising, U. Scherf, K. Müllen, Physical Review B 57 (1998) R4202–R4205.
[38] S. Barth, H. Bässler, Physical Review Letters 79 (1997) 4445–4448.
[39] M. Pope, C.E. Swenberg, Electronic Processes in Organic Crystals and Polymers, Oxford University Press, Oxford, UK, 1999.
[40] B. Schweitzer, H. Bässler, Synthetic Metals 109 (2000) 1–6.
[41] D. Moses, J. Wang, A.J. Heeger, N. Kirova, S. Brazovski, Proceedings of the National academy of Sciences of the United States of America 98 (2001) 13496–13500.
[42] J.-M. Nunzi, Physique 3 (2002) 523–542.
[43] D. Wöhrle, D. Meissner, Advanced Materials 3 (1991) 129.
[44] G.A. Chamberlain, Solar Cells 8 (1983) 47.
[45] C.J. Brabec, N.S. Sariciftci, J.C. Hummelen, Advanced Functional Materials 11 (2001) 15–26.
[46] C.J. Brabec, Chemical Physics Letters 240 (2001) 232.
[47] N.S. Sariciftci, L. Smilowitz, A.J. Heeger, F. Wudl, Science 258 (1992) 1474–1476.
[48] C.W. Tang, Applied Physics Letters 48 (1986) 183–185.
[49] G. Yu, A.J. Heeger, Journal of Applied Physics 78 (1995) 4510–4515.
[50] J.J.M. Halls, N.C. Walsh, E.A. Greenham, E.A. Marseglia, R.H. Friend, S.C. Moratti, A.B. Holmes, Nature 376 (1995) 498–500.
[51] B.R. Saunders, M.L. Turner, Advances in Colloid and Interface Science 138 (2008) 1–23.
[52] H. Spanggaard, F.C. Krebs, Solar Energy Materials and Solar Cells 83 (2004) 125–146.
[53] M.M. Wienk, J.M. Kroon, W.J.H. Verhees, J. Knol, J.C. Hummelen, P.A. van Hal, R.A.J. Janssen, Angewandte Chemie International Edition 42 (2003) 3371–3375.
[54] A. Hadipour, B. de Boer, P.W.M. Blom, Advanced Functional Materials 18 (2008) 169–181.
[55] S. Sista, Z. Hong, L.-M. Chen, Y. Yang, Energy Environ Sci (2011). online article.
[56] L.A.A. Pettersson, L.S. Roman, O. Inganäs, Journal of Applied Physics 86 (1999) 487–496.
[57] J.J.M. Halls, K. Pichler, R.H. Friend, S.C. Moratti, A.B. Holmes, Applied Physics Letters 68 (1996) 3120–3122.
[58] V.D. Mihailetchi, L.J.A. Koster, P.W.M. Blom, Applied Physics Letters 85 (2004) 970–972.
[59] H. Hoppe, T. Glatzel, M. Niggeman, M. Schwinger, F. Schaeffler, A. Hinsch, M.C. Lux-Steiner, N.S. Sariftci, Thin Solid Fillms 511–512 (2006) 587.
[60] H. Hoppe, N.S.J. Sariciftci, Journal of Materials Chemistry 16 (2006) 45–61.
[61] V. Coropceanu, J. Cornil, D.A. da Silva Filho, Y. Olivier, R. Silbey, J.-L. Brédas, Chemical Reviews 107 (2007) 926–952.
[62] J. Hwang, A. Wan, A. Kahn, Materials Science and Engineering Reports 64 (2009) 1–31.
[63] J.C. Hummelen, B.W. Knight, F. LePeq, F. Wudl, Journal of Organic Chemistry 60 (1995) 532–538.
[64] F. Padinger, R.S. Rittberger, N.S. Sariciftci, Advanced Functional Materials 13 (2003) 85–88.
[65] C. Waldauf, P. Schilinsky, J.A. Hauch, C.J. Brabec, Thin Solid Films 451–452 (2004) 503–507.
[66] M. Reyes-Reyes, K. Kim, D.L. Carroll, Applied Physics Letters 87 (2005) 083506.
[67] X. Yang, J. Loos, Macromolecules 40 (2007) 1353–1362.
[68] M. Al-Ibrahim, O. Ambacher, S. Sensfuss, G. Gobsch, Applied Physics Letters 86 (2005) 201120.
[69] S.E. Shaheen, C.J. Brabec, N.S. Sariciftci, F. Padinger, T. Fromherz, J.C. Hummelen, Applied Physics Letters 78 (2001) 841–843.
[70] A.J. Mozer, P. Denk, M.C. Scharber, H. Neugebauer, N.S. Sariciftci, P. Wagner, L. Lutsen, D. Venderzande, Journal of Physical Chemistry B 108 (2004) 5235–5242.
[71] J. Roncali, Chemical Reviews 92 (1992) 711–738.
[72] R.D. McCullough, Advanced Materials 10 (1998) 93–116.
[73] A. Seeman, H.-J. Egelhaaf, C.J. Brabec, J.A. Hauch, Organic Electronics 10 (2009) 1424–1428.
[74] L. Moro, R.J. Visser, Barrier Films for Photovoltaics, in: C.J. Brabec, V. Dyakonov, U. Scherf (Eds.), Organic Photovoltaics – Materials, Device Physics, and Manufacturing Technologies, Wiley-VCH, Weinheim, 2008.
[75] (http://www.corning.com/displaytechnologies/en/products/flexible.aspx).
[76] V.D. Mihailetchi, L.J.A. Koster, J.C. Hummelen, P.W.M. Blom, Physical Review Letters 93 (2004). 216601-216601/216604.
[77] J. Guo, H. Ohkita, H. Benten, S. Ito, Journal of the American Chemical Society 132 (2010) 6154–6164.
[78] L.J.A. Koster, V.D. Mihailetchi, R. Ramaker, P.W.M. Blom, Applied Physics Letters 86 (2005) 123509.
[79] A. Miller, E. Abrahams, Physical Reviews 12 (1960) 745–755.
[80] J. Stephan, S. Schraber, L. Brehmer, Synthetic Metals 111–112 (2000) 353–357.
[81] M.S.A. Abdou, S. Holdcroft, Macromolecules 26 (1993) 2954–2962.
[82] M.S.A. Abdou, M.S.A. Abdou, M.S.A. Abdou, M.S.A. Abdou, G.A. Diaz-Guijada, M.I. Arroyo, S. Holdcroft, Chemistry of Materials 3 (1991) 1003–1006.
[83] M. Manceau, A. Rivaton, J.-L. Gardette, S. Guillerez, N. Lemaître, Polymer Degradation and Stability 94 (2009) 898–907.
[84] M. Manceau, A. Rivaton, J.-L. Gardette, Macromolecular Rapid Communications 29 (2008) 1823–1827.
[85] R. Pacios, A.J. Chatten, K. Kawano, J.R. Durrant, D.D.C. Bradley, J. Nelson, Advanced Functional Materials 16 (2006) 2117–2126.
[86] H. Hintz, H.-J. Egelhaaf, L. Lüer, J.A. Hauch, H. Peisert, T. Chassé, Chemistry of Materials 23 (2011) 145–154.
[87] M. Manceau, E. Bundgaard, J.E. Carlé, O. Hagemann, M. Helgesen, R. Søndergaard, M. Jørgensen, F.C. Krebs, Journal of Materials Chemistry 21 (2011) 4132–4141.
[88] A. Rivaton, S. Chambon, M. Manceau, J.-L. Gardette, N. Lemaître, S. Guillerez, Polymer Degradation and Stability 95 (2010) 278–284.
[89] M. Manceau, S. Chambon, A. Rivaton, J.-L. Gardette, S. Guillerez, N. Lemaître, Solar Energy Materials and Solar Cells 94 (2010) 1572–1577.
[90] H. Neugebauer, C.J. Brabec, J.C. Hummelen, N.S. Sariciftci, Solar Energy Materials and Solar Cells 61 (2000) 35–42.
[91] S. Chambon, A. Rivaton, J.-L. Gardette, M. Firon, Solar Energy Materials and Solar Cells 92 (2008) 785–792.
[92] H.W. Sarkas, W. Kwan, S.R. Flom, C.D. Merritt, Z.H. Kafafi, Journal of Physical Chemistry 100 (1996) 5169–5171.
[93] T.D. Anthropoulos, T.S. Shafai, Thin Solid Films 441 (2003) 207–213.
[94] E.J. Meijer, A.V.G. Mangnus, B.-H. Huisman, G.W. 't Hooft, D.M. de Leeuw, T.M. Klapwijk, Synthetic Metals 142 (2004) 53–56.
[95] M.S.A. Abdou, F.P. Orfino, Y. Son, S. Holdcroft, Journal of the American Chemical Society 119 (1997) 4518–4524.
[96] H.-J. Egelhaaf, L. Lüer, D. Oelkrug, G. Winter, P. Haisch, M. Hanack, Synthetic Metals 84 (1997) 897–898.
[97] L. Lüer, H.-J. Egelhaaf, D. Oelkrug, G. Cerullo, G. Lanzani, B.-H. Huisman, D. de Leeuw, Organic Electronics 5 (2004) 83–89.
[98] H.-H. Liao, C.-M. Yang, C.-C. Liu, S.-F. Horng, H.-F. Meng, J.-T. Shy, Journal of Applied Physics 103 (2008) 104506.
[99] N.C. Billingham, P.D. Calvert, P.J.S. Foot, F. Mohammad, Polymer Degradation and Stability 19 (1987) 323–341.
[100] M.S.A. Abdou, S. Holdcroft, Chemistry of Materials 6 (1994) 962–968.
[101] T.D. Nielsen, K. Bechgaard, F.C. Krebs, Macromolecules 38 (2005) 658–659.
[102] T.D. Nielsen, K. Bechgaard, F.C. Krebs, Synthesis 10 (2006) 1639–1644.
[103] Z. Liang, A. Nardes, D. Wang, J.J. Berry, B.A. Gregg, Chemistry of Materials 21 (2009) 4914–4919.
[104] Z. Liang, M.O. Reese, B.A. Gregg, A.C.S. Appl, Mater Interfaces 3 (2011) 2042–2050.
[105] J. Milliken, T.M. Keller, A.P. Baronavski, S.W. McElvany, J.H. Callahan, H.H. Nelson, Chemistry of Materials 3 (1991) 386–387.
[106] I.M.K. Ismail, Carbon 30 (1992) 229–239.
[107] A. Tapponnier, I. Biaggio, P. Günter, Applied Physics Letters 86 (2005) 112114.

[108] A. Hamed, Y.Y. Sun, Y.K. Tao, R.L. Meng, P.H. Hor, Physical Review B 47 (1993) 10875–10880.
[109] P.C. Eklund, A.M. Rao, P. Zhou, Y. Wang, J.M. Holden, Thin Solid Films 257 (1995) 185–203.
[110] J.W. Arbogast, A.P. Darmanyan, C.S. Foote, Y. Rubin, F.N. Diederich, M.M. Alvarez, S.J. Anz, R.L. Whetten, Journal of Physical Chemistry 95 (1991) 11–12.
[111] K.M. Creegan, J.L. Robbins, W.K. Robbins, J.M. Millar, R.D. Sherwood, P.J. Tindall, D.M. Cox, Journal of the American Chemical Society 114 (1992) 1103–1105.
[112] G.H. Kroll, P.J. Benning, Y. Chen, T.R. Ohno, M.S. Weaver, L.P.F. Chibante, R.E. Smalley, Chemical Physics Letters 181 (1991) 112–116.
[113] R. Lessmann, Z. Hong, S. Scholz, B. Maennig, M.K. Riede, K. Leo, Organic Electronics 11 (2010) 539–543.
[114] M. Wohlers, H. Werner, D. Herein, T. Schedel-Niedrig, A. Bauer, R. Schlögl, Synthetic Metals 77 (1996) 299–302.
[115] K. Norrman, N.B. Larsen, F.C. Krebs, Solar Energy Materials and Solar Cells 90 (2006) 2793–2814.
[116] R. Könenkamp, G. Priebe, B. Pietzak, Physical Review B 60 (1999) 11804–11808.
[117] J.K.J. van Duren, X. Yang, J. Loos, C.W.T. Bulle-Lieuwma, A.B. Sieval, J.C. Hummelen, R.A.J. Janssen, Advanced Functional Materials 14 (2004) 425–433.
[118] D. Chirvase, J. Parisi, J.C. Hummelen, V. Dyakonov, Nanotechnology 15 (2004) 1317–1323.
[119] M. Urien, L. Bailly, L. Vignau, E. Cloutet, A. de Cuendias, G. Wants, H. Cramail, L. Hirsch, J.-P. Parneix, Polymer International 57 (2008) 764–769.
[120] S. Kim, S. Cook, S.M. Tuladhar, S.A. Choulis, J. Nelson, J.R. Durrant, D.D.C. Bradley, M. Giles, I. McCulloch, C.-S. Ha, M. Ree, Nature Materials 5 (2006) 197–203.
[121] W.-H. Baek, H. Yang, T.-S. Yoon, C.J. Kang, H.H. Lee, Y.-S. Kim, Solar Energy Materials and Solar Cells 93 (2009) 1263–1267.
[122] A. Zen, M. Saphiannikova, D. Neher, J. Grenzer, S. Grigorian, U. Pietsch, U. Asawapirom, S. Janietz, U. Scherf, I. Lieberwirth, G. Wegner, Macromolecules 39 (2006) 2162–2171.
[123] L. Zeng, C.W. Tang, S.H. Chen, Applied Physics Letters 97 (2010) 053305.
[124] M.K. Riede, K.O. Sylvester-Hvid, M. Clatthaar, N. Keegan, T. Ziegler, B. Zimmermann, M. Niggeman, A.W. Liehr, G. Willeke, A. Gombert, Progress in Photovoltaics: Research and Applications 16 (2008) 561.
[125] P. Vanlaeke, G. Vanhoyland, T. Aernouts, D. Cheyns, C. Deidel, J. Manca, P. Heremans, J. Poortmans, Thin Solid Fillms 511–512 (2006) 358–361.
[126] V.D. Mihailetchi, H. Xie, B. de Boer, L.J.A. Koster, P.W.M. Blom, Advanced Functional Materials 16 (2006) 699–708.
[127] J. Jo, S.-S. Kim, S.-I. Na, B.-K. Yu, D.-Y. Kim, Advanced Functional Materials 19 (2009) 866–874.
[128] J. Zhao, A. Swinnen, G. Van Assche, J. Manca, D. Vanderzande, B. van Mele, Journal of Physical Chemistry B 113 (2009) 1587–1591.
[129] B. Watts, W.J. Belcher, L. Thomsen, H. Ade, P.C. Dastoor, Macromolecules 42 (2009) 8392–8397.
[130] H. Hoppe, M. Niggeman, C. Winder, J. Kraut, R. Hiesgen, A. Hinsch, D. Meissner, N.S. Sariciftci, Advanced Functional Materials 14 (2004) 1005–1011.
[131] X. Yang, J.K.J. Van Duren, R.A.J. Janssen, M.A.J. Michels, J. Loos, Macromolecules 37 (2004) 2152–2158.
[132] B. Conings, S. Bertho, K. Vandewal, A. Senes, J. D'Haen, J. Manca, R.A.J. Janssen, Applied Physics Letters 96 (2010) 163301.
[133] E. Klimov, W. Li, X. Yang, G.G. Hoffmann, J. Loos, Macromolecules 39 (2006) 4493–4496.
[134] S. van Bavel, 3D Morphology of Photoactive Layers of Polymer Solar Cells, in: vol Ph. D. thesis, 3D Morphology of Photoactive Layers of Polymer Solar Cells, Eindhoven University of Technology, Eindhoven, the Netherlands, 2009.
[135] J. Peet, J.Y. Kim, N.E. Coates, W.L. Ma, D. Moses, A.J. Heeger, G.C. Bazan, Nature Materials 6 (2007) 497–500.
[136] L. Li, G. Lu, X. Yang, Journal of Materials Chemistry 18 (2008) 1984–1990.
[137] A.J. Moulé, K. Meerholz, Advanced Functional Materials 19 (2009) 3028–3036.
[138] W. Wang, H. Wu, C. Yang, C. Luo, Y. Zhang, J. Chen, Y. Cao, Applied Physics Letters 90 (2007) 183512.
[139] G. Li, V. Shrotriya, Y. Yao, J. Huang, Y. Yang, Journal of Materials Chemistry 17 (2007) 3126–3140.
[140] K. Bücher, Solar Energy Materials and Solar Cells 47 (1997) 85–94.
[141] H. Hänsel, H. Zettl, G. Krausch, C. Schmitz, R. Kisselev, M. Thelakkat, H.-W. Schmidt, Applied Physics Letters 81 (2002) 2106–2108.
[142] G. TamizhMani, Photovolt. Int. 8 (2010) 146–152.
[143] S. Bertho, G. Janssen, T.J. Cleij, B. Conings, W. Moons, A. Gadisa, J. D'Haen, E. CGoovaerts, L. Lutsen, J. Manca, D. Vanderzande, Solar Energy Materials and Solar Cells 92 (2008) 753–760.
[144] G. Kalita, M. Masahiro, W. Koichi, M. Umeno, Solid-State Electronics 54 (2010) 447–451.
[145] W.L. Ma, C. Yang, X. Gong, K. Lee, A.J. Heeger, Advanced Functional Materials 15 (2005) 1617–1622.
[146] S. Bertho, I. Haeldermans, A. Swinnen, W. Moons, T. Martens, L. Lutsen, D. Vanderzande, J. Manca, A. Senes, A. Bonfiglio, Solar Energy Materials and Solar Cells 91 (2007) 385–389.
[147] J.C. Hindson, B. Ulgut, R.H. Friend, E.A. Greenham, B. Norder, A. Kotlewski, T.J. Dingemans, Journal of Materials Chemistry 20 (2010) 937–944.
[148] K. Sivula, Z.T. Ball, N. Watanabe, J.M.J. Fréchet, Advanced Materials 19 (2009) 206–210.
[149] B.J. Kim, Y. Miyamoto, B. Ma, J.M.J. Fréchet, Advanced Functional Materials 19 (2009) 2273–2281.
[150] M. Drees, H. Hoppe, C. Winder, H. Neugebauer, N.S. Sariciftci, M. Schwinger, F. Schäffler, C. Topf, M.C. Scharber, Z. Zhu, R. Gaudiana, Journal of Materials Chemistry 15 (2005) 5158–5163.
[151] S. Miyanishi, K. Tajima, K. Hashimoto, Macromolecules 42 (2009) 1610–1618.
[152] F. Giacalone, N. Martín, Advanced Materials 22 (2010) 4220–4248.
[153] A. Marcos Ramos, M.T. Rispens, K.J. van Duren, J.C. Hummelen, R.A.J. Janssen, Journal of the American Chemical Society 123 (2001) 6714–6715.
[154] N. Sary, F. Richard, C. Brochon, N. Leclerc, P. Lévêque, J.-N. Audinot, S. Berson, T. Heiser, G. Hadziioannou, R. Mezzenga, Advanced Materials 22 (2010) 763–768.
[155] M. Sommer, S. Hüttner, U. Steiner, M. Thelakkat, Applied Physics Letters 95 (2009) 183308.
[156] C. Guillén, J. Herrero, High-Performance Electrodes for Organic Photovoltaics, in: C.J. Brabec, V. Dyakonov, U. Scherf (Eds.), Organic Photovoltaics – Materials, Device Physics, and Manufacturing Technologies, Wiley-VCH, Weinheim, 2008.
[157] D.C. Choo, H.C. Im, D.U. Lee, T.W. Kim, J.W. Han, E.H. Choi, Solid State Communications 136 (2005) 365–368.
[158] T. Taima, M. Chikamatsu, Y. Yoshida, K. Saito, K. Yase, IEICE: Transactions on Electronics E87C (2004) 2045–2048.
[159] M.O. Reese, M.S. White, G. Rumbles, D.S. Ginley, S.E. Shaheen, Applied Physics Letters 92 (2008) 053307.
[160] M.T. Llyod, D.C. Olson, P. Lu, E. Fang, D.L. Moore, M.S. White, M.O. Reese, D.S. Ginley, J.W.P. Hsu, Journal of Materials Chemistry 19 (2009) 7638–7642.
[161] K. Kawano, R. Pacios, D. Poplavskyy, J. Nelson, D.D.C. Bradley, J.R. Durrant, Solar Energy Materials and Solar Cells 90 (2006) 3520–3530.
[162] B. Paci, A. Generosi, V.R. Albertini, P. Perfetti, R. de Bettignies, J. Leroy, M. Firon, C. Sentein, Applied Physics Letters 89 (2006) 043507.
[163] B. Paci, A. Generosi, V.R. Albertini, P. Perfetti, M. Firon, J. Leroy, C. Sentein, Applied Physics Letters 87 (2005) 194110.
[164] H. Klauk, J.R. Huang, J.A. Nichols, T.N. Jackson, Thin Solid Fillms 366 (2000) 272–278.
[165] J.W. Lim, M. Isshiki, Journal of Applied Physics 99 (2006) 094909.
[166] K. Norrman, F.C. Krebs, Solar Energy Materials and Solar Cells 90 (2006) 213–227.
[167] K. Norrman, A. Gevorgyan, F.C. Krebs, Applied Materials Interfaces 1 (2009) 102.
[168] M.O. Reese, A.J. Morfa, M.S. White, N. Kopidakis, S.E. Shaheen, G. Rumbles, D.S. Ginley, Solar Energy Materials and Solar Cells 92 (2008) 746–752.
[169] T. Jeranko, H. Tributsch, S.N. Sariciftci, J.C. Hummelen, Solar Energy Materials and Solar Cells 83 (2004) 247–262.
[170] F.C. Krebs, J.E. Carlé, N. Cruys-Bagger, M. Andersen, M.R. Lilliedal, M.A. Hammond, S. Hvidt, Solar Energy Materials and Solar Cells 86 (2005) 499–516.
[171] U.K. Barik, S. Srinivasan, C.L. Nagendra, A. Subrahmanyam, Thin Solid Films 429 (2003) 129–134.
[172] F.C. Krebs, A. Gevorgyan, J. Alstrup, Journal of Materials Chemistry 19 (2009) 5442–5551.
[173] C. Girotto, B.P. Rand, S. Steudel, A. Hadipour, T. Aernouts, J. Genoe, P. Heremans, Spray-coating as a deposition technique for fully solution processed polymer solar cells, in: 24th European Photovolataic Solar Energy Conference, Hamburg, Germany, 2009.
[174] W. Song, Z. Li, S.K. So, Y. Qiu, Y. Zhu, L. Cao, Surface and Interface Analysis 32 (2001) 102–105.
[175] W. Song, S.K. So, J. Moulder, Y. Qiu, Y. Zhu, L. Cao, Surface and Interface Analysis 32 (2001) 70–73.

[176] H.M. Grandin, S.M. Tadayyon, W.N. Lennard, K. Griffiths, L.L. Coastsworth, P.R. Norton, Z.D. Popovic, H. Aziz, N.X. Hu, Organic Electronics 4 (2003) 9–14.
[177] Y.J. Suh, S.Y. Park, T.H. Lee, W.S. Chung, K.K. Kim, M.J. Kim, Microsc. Microanal. 16 (Suppl. 2) (2010) 1378–1379.
[178] J.C. Manifacier, Thin Solid Fillms 90 (1982) 297–308.
[179] T. Minami, Semiconductor Science and Technology 20 (2005) S35–S44.
[180] I.A. Rauf, Journal of Applied Physics 79 (1996) 4057–4065.
[181] J.S. Kim, R.H. Friend, F. Cacialli, Journal of Applied Physics 86 (1999) 2774–2778.
[182] N.R. Armstrong, C. Carter, C. Donley, A. Simmonds, P. Lee, M. Brumbach, B. Kippelen, B. Domercq, S. Yoo, Thin Solid Films 445 (2003) 342–352.
[183] P. Peumans, S.R. Forrest, Applied Physics Letters 79 (2001) 126–128.
[184] K. Book, H. Bässler, A. Elschner, S. Kirchmeyer, Organic Electronics 4 (2003) 227–232.
[185] V. Shrotriya, G. Li, Y. Yao, C.-W. Chu, Y. Yang, Applied Physics Letters 88 (2006) 073508.
[186] F. Nüesch, T. G, L. Zuppiroli, F. Meng, K.X. Chen, H. Tian, Solar Energy Materials and Solar Cells 87 (2005) 817–824.
[187] I. Yoo, M. Lee, C. Lee, D.-W. Kim, I.S. Moon, S.-H. Hwang, Synthetic Metals 153 (2005) 97–100.
[188] C.H.L. Weijtens, V. van Elsbergen, M.M. De Kok, S.H.P.M. de Winter, Organic Electronics 6 (2005) 97–104.
[189] M.P. de Jong, A.W. Denier van der Gon, X. Crispin, W. Osikowicz, W.R. Salaneck, L. Groenendaal, J. Chem. Phys. 118 (2003) 6495–6502.
[190] A. Petr, F. Zhang, H. Peisert, M. Knupfer, L. Dunsch, Chemical Physics Letters 385 (2004) 140–143.
[191] V. Djara, J.C. Bernède, Thin Solid Films 493 (2005) 273–277.
[192] F.Z. Dahou, L. Cattin, J. Garnier, J. Ouerfelli, M. Morsli, G. Louarn, A. Bouteville, A. Khellil, J.C. Bernède, Thin Solid Films 518 (2010) 6117–6122.
[193] M.P. de Jong, L.J. van IJzendoorn, M.J.A. de Voigt, Applied Physics Letters 77 (2000) 2255–2257.
[194] A.M. Nardes, M. Kemerink, M.M. de Kok, E. Vinken, K. Maturova, R.A.J. Janssen, Organic Electronics 9 (2008) 727–734.
[195] C.W.T. Bulle-Lieuwma, W.J.H. van Gennip, J.K.J. van Duren, P. Jonkheijm, R.A.J. Janssen, J.W. Niemantsverdriet, Applied Surface Science 203–204 (2003) 547–550.
[196] C.W.T. Bulle-Lieuwma, J.K.J. van Duren, X. Yang, J. Loos, A.B. Sieval, J.C. Hummelen, R.A.J. Janssen, Applied Surface Science 231–232 (2004) 274–277.
[197] G.-F. Wang, X.-M. Tao, R.-X. Wang, Nanotechnologies 19 (2008) 145201.
[198] A.J. Medford, M.R. Lilliedal, M. Jørgensen, D. Aarø, H. Pakalski, J. Fyenbo, F.C. Krebs, Optics Express 18 (2010) A272–A285.
[199] C.C. Wu, C.I. Wu, J.C. Sturm, A. Kahn, Applied Physics Letters 70 (1997) 1348–1350.
[200] B.H. Cumpston, I.D. Parker, K.F. Jensen, Journal of Applied Physics 81 (1997) 3716–3720.
[201] M.M. de Kok, M. Buechel, S.I.E. Vulto, P. van de Weijer, E.A. Meulenkamp, S.H.P.M. de Winter, A.J.G. Mank, H.J.M. Vorstenbosch, C.H.L. Weijtens, V. van Elsbergen, Phys. Stat. Sol. a 201 (2004).
[202] S. Karg, J.C. Scott, J.R. Salem, M. Angelopoulos, Synthetic Metals 80 (1996) 111–117.
[203] G. Gustafsson, G.M. Treacy, Y. Cao, F. Klavetter, N. Colaneri, A.J. Heeger, Synthetic Metals 55–57 (1993) 4123–4127.
[204] A. M. Nardes, in: vol Ph. D. thesis, Ph.D. thesis, On the conductivity of PEDOT:PSS thin films, Eindhoven University of Technology, Eindhoven, the Netherlands, 2007.
[205] F.C. Krebs, Solar Energy Materials and Solar Cells 93 (2009) 1636–1641.
[206] E. Rubingh, P. Kruijt, R. Andriessen, Towards TCO-less large area OLEDs for lighting applications, in: Proceedings of LOPE-C conference, Francfort, Germany, 2009.
[207] S.-I. Na, S.-S. Kim, J. Jo, D.-Y. Kim, Advanced Materials 20 (2008) 4061–4067.
[208] K. Tvingstedt, O. Inganäs, Advanced Materials 19 (2007) 2893–2897.
[209] T. Aernouts, P. Vanlaeke, W. Geens, J. Poortmans, P. Heremans, S. Borghs, R. Mertens, R. Andriessen, L. Leenders, Thin Solid Films 451–452 (2004) 22–25.
[210] M. Glatthaar, M. Niggemann, B. Zimmermann, P. Lewer, M. Riede, A. Hinsch, J. Luther, Thin Solid Films 491 (2005) 298–300.
[211] Y. Galagan, J.-E.J.M. Rubingh, R. Andriessen, C.-C. Fan, P.W.M. Blom, S.C. Veenstra, J.M. Kroon, Solar Energy Materials and Solar Cells 95 (2010) 1339–1343.
[212] B. Zimmermann, M. Glatthaar, M. Niggemann, M. Riede, A. Hinsch, A. Gombert, Solar Energy Materials and Solar Cells 91 (2007) 374–378.
[213] J. Zou, H.-L. Yip, S.K. Hau, A.K.-Y. Jen, Applied Physics Letters 96 (2010) 203301.
[214] O. Inganäs, Nature Photonics 5 (2011) 201–202.
[215] B. O'Connor, C. Haughn, K.-H. An, K.P. Pipe, M. Shtein, Applied Physics Letters 93 (2008) 223304.
[216] C.-Y. Su, A.-Y. Lu, Y.-L. Chen, C.-Y. Wei, C.-H. Weng, P.-C. Wang, F.-R. Chen, K.-C. Leou, C.-H. Tsai, Journal of Physical Chemistry C 114 (2010) 11588–11594.
[217] M. Choe, B.H. Lee, G. Jo, J. Park, W. Park, S. Lee, W.-K. Hong, M.-J. Seong, Y.H. Kahng, K. Lee, T. Lee, Organic Electronics 11 (2010) 1864–1869.
[218] C.J. Brabec, S.E. Shaheen, C. Winder, N.S. Sariciftci, Applied Physics Letters 80 (2002) 1288–1290.
[219] Y. Wang, L. Yang, C. Yao, W. Qin, S. Yin, F. Zhang, Solar Energy Materials and Solar Cells 95 (2011) 1243–1247.
[220] L. Yang, H. Xu, H. Tian, S. Yin, F. Zhang, Solar Energy Materials and Solar Cells 94 (2010) 1831–1834.
[221] G. Dennler, C. Lungenschmied, H. Neugebauer, N.S. Sariciftci, A. Labouret, Journal of Materials Research 20 (2005) 3224–3233.
[222] J.A. Hauch, P. Schilinsky, S.A. Choulis, S. Rajoelson, C.J. Brabec, Applied Physics Letters 93 (2008) 103306.
[223] S. Cros, R. De Bettignies, S. Berson, S. Bailly, P. Maisse, N. Lemaitre, S. Guillerez, Solar Energy Materials and Solar Cells 95 (2011) S65–S69.
[224] J.A. Hauch, P. Schilinsky, S.A. Choulis, R. Childers, M. Biele, C.J. Brabec, Solar Energy Materials and Solar Cells 92 (2008) 727–731.
[225] F. van Assche, H. Rooms, E. Young, J. Michels, T. van Mol, G. Rietjens, P. Van de Weijer, P. Bouten, Proceedings 22nd AIMCAL Fall Technical Conference, Myrtle Beach, SC (October 19-22, 2008).
[226] A.M.B. van Mol, P. Van de Weijer, C. Tanase, Proceedings of SPIE 6999 (2008) 46.
[227] K. Norrman, M.V. Madsen, S.A. Gevorgyan, F.C. Krebs, Journal of the American Chemical Society 132 (2010) 16883–16892.
[228] A.G. Erlat, R.J. Spontak, R.P. Clarke, T.C. Robinson, P.D. Haaland, Y. Tropsha, N.G. Harvey, E.A. Vogler, Journal of Physical Chemistry B 103 (1999) 6047–6055.
[229] G. Dennler, C. Lungenschmied, H. Neugebauer, N.S. Sariciftci, M. Latreche, G. Czeremuszkin, M.R. Wertheimer, Thin Solid Films 511–512 (2006) 349–353.
[230] J.D. Affinito, M.E. Gross, C.A. Coronado, G.L. Graff, E.N. Greenwell, P.M. Martin, Thin Solid Films 290–291 (1996) 63–67.
[231] T.W. Kim, M. Yan, A.G. Erlat, P.A. McConnelee, M. Pellew, J. Deluca, T.P. Feist, A.R. Duggal, M. Schaepkens, Journal of Vacuum Science & Technology A. 23 (2005) 971–977.
[232] M. Schaepkens, T.W. Kim, A.G. Erlat, M. Yan, K.W. Flanagan, C.M. Heller, P.A. McConnelee, Journal of Vacuum Science & Technology, A: Vacuum, Surfaces, and Films 22 (2004) 1716–1722.
[233] G.L. Graff, R.E. Williford, P.E. Burrows, Journal of Applied Physics 96 (2004) 1840–1849.
[234] A.A. Abdallah, In: Mechanical integrity of multi-layered structures for flexible displays, Eindhoven University of Technology, Eindhoven, the Netherlands, 2007.
[235] G.M. Wallner, C. Weigl, R. Leitgeb, R.W. Lang, Polymer Degradation and Stability 85 (2004) 1065–1070.
[236] J.S. Lewis, M.S. Weaver, IEEE Journal of Selected Topics in Quantum Electronics 10 (2004) 45–57.
[237] J.R. White, Comptes Rendus Chimie 9 (2006) 1396–1408.
[238] G.M. Wallner, R.W. Lang, Solar Energy 79 (2005) 603–611.
[239] M. Day, D.M. Wiles, Journal of Applied Polymer Science 16 (1972) 191–202.
[240] W.A. MacDonald, Flexible Substrates Requirements for Organic Photovoltaics, in: F.C. Krebs, V. Dyakonov, U. Scherf (Eds.), Organic Photovoltaics – Materials, Device Physics, and Manufacturing Technologies, Wiley-VCH, Weinheim, 2008.
[241] F.C. Krebs, Solar Energy Materials and Solar Cells 92 (2008) 715–726.
[242] C. Lungenschmied, G. Dennler, H. Neugebauer, S.N. Sariciftci, M. Glatthaar, T. Meyer, A. Meyer, Solar Energy Materials and Solar Cells 91 (2007) 379–384.
[243] C. Jonda, A.B.R. Mayer, U. Stolz, A. Elschner, A. Karbach, Journal of Materials Science 35 (2000) 5645–5651.
[244] S.A. Gevorgyan, A.J. Medford, E. Bundgaard, S.B. Sapkota, H.-F. Schleiermacher, B. Zimmermann, U. Würfel, A. Chafiq, M. Lira-Cantu, T. Swonke, M. Wagner, C.J. Brabec, O. Haillant, E. Voroshazi, T. Aernouts, R. Steim, J.A. Hauch, A. Elschner, M. Pannone, M. Xiao, A. Langzettel, D. Laird, M.T. Lloyd, T. Rath, E. Maier, G. Trimmel, M.

Hermenau, T. Menke, K. Leo, R. Rösch, M. Seeland, H. Hoppe, T.J. Nagle, K.B. Burke, C.J. Fell, D. Vak, T.B. Singh, S.E. Watkins, Y. Galagan, A. Manor, E.A. Katz, T. Kim, K. Kim, P.M. Sommeling, W.J.H. Verhees, S.C. Veenstra, M. Riede, M.G. Christoforo, T. Currier, V. Shrotriya, G. Schwartz, F.C. Krebs, Solar Energy Materials and Solar Cells 95 (2011) 1398–1416.
[245] F.C. Krebs, T.D. Nielsen, J. Fyenbo, M. Wadstrøm, M.S. Pedersen, Energy & Environmental Science 3 (2010) 512–525.
[246] R. Steim, P. Schilinsky, S.A. Choulis, C.J. Brabec, Solar Energy Materials and Solar Cells 93 (2009) 1963–1967.
[247] P.E. Burrows, V. Vulovic, S.R. Forrest, L.S. Sapochak, D.M. McCarty, M.E. Thompson, Applied Physics Letters 65 (1994) 2922–2924.
[248] F.C. Krebs, R.B. Nyberg, M. Jørgensen, Chemistry of Materials 16 (2004) 1313–1318.
[249] D.L. King, M.A. Quintana, J.A. Kratochvil, D.E. Ellibee, B.R. Hansen, Progress in Photovoltacis 8 (2000) 241.
[250] R. Steim, S.A. Choulis, P. Schilinsky, U. Lemmer, C.J. Brabec, Applied Physics Letters 94 (2009) 043304.
[251] F.C. Krebs, M. Jørgensen, K. Norrman, O. Hagemann, J. Alstrup, T.D. Nielsen, J. Fyenbo, K. Larsen, J. Kristensen, Solar Energy Materials and Solar Cells 93 (2009) 422–441.
[252] E.D. Dunlop, D. Halton, H.A. Ossenbrink, IEEE Proceedings (2005) 1593–1596.
[253] Y. Meydbray, K. Wilson, E. Brambila, A. Terao, S. Daroczi, Proceedings of European Photovoltaic Solar Energy Conferences (2007) 2561–2564.
[254] R. Jones, T. Johnson, W. Jordan, S. Wagner, J. Yang, S. Guha, IEEE Proceedings (2002) 1214–1217.
[255] T.J. McMahon, Progress in Photovoltaics: Research and Application 11 (2004) 225–230.
[256] O. Haillant, Accelerated Weathering Testing to Predict the Environmental Durability of Organic Systems, in: Conference proceedings of the 25th European Photovoltaic Solar Energy Conference and Exhibition/5th World Conference on Photovoltaic Energy Conversion, Valencia, Spain, 2010. pp. 3952–3959.
[257] M.R. Lilliedal, A.J. Medford, M.V. Madsen, K. Norrman, F.C. Krebs, Solar Energy Materials and Solar Cells 12 (2010) 2018–2031.
[258] M.S. Arnold, P. Avouris, Z.W. Pan, Z.L. Wang, Journal of Physical Chemistry B 107 (2003) 659–663.
[259] (http://isosconference.org/)
[260] H. Hoppe, J. Bachmann, B. Muhsin, K.-H. Drüe, I. Riedel, G. Gobsch, C. Buerhop-Lutz, C.J. Brabec, V. Dyakonov, Journal of Applied Physics 107 (2010) 014505.
[261] F. Padinger, T. Fromherz, P. Denk, C.J. Brabec, J. Zettner, T. Hierl, S.N. Sariciftci, Synthetic Metals 121 (2001) 1605–1606.
[262] S.S. van Bavel, E. Sourty, G. de With, J. Loos, Nano Letters 9 (2009) 507–513.
[263] J. Loos, J.K.J. Van Duren, F. Morrissey, R.A.J. Janssen, Polymer 43 (2002) 7493–7496.
[264] M. Glatthaar, M. Riede, N. Keegan, K. Sylvester-Hvid, B. Zimmermann, M. Niggemann, A. Hinsch, A. Gombert, Solar Energy Materials and Solar Cells 91 (2007) 390–393.
[265] D.G.J. Sutherland, J.A. Carlisle, P. Elliker, G. Fox, T.W. Hagler, I. Jimenez, H.W. Lee, K. Pakbaz, L.J. Terminello, S.C. Williams, Applied Physics Letters 68 (1996) 2046–2048.